

Cyclooctatetraene (COT)-Coordinated Diiron Carbene Complexes and Their Remarkable Thermolysis Reactions[†]

Lei Zhang,[‡] Shu Zhang,[‡] Qiang Xu,^{*,§} Jie Sun,[‡] and Jiabi Chen^{*,‡}

State Key Laboratory of Organometallic Chemistry, Shanghai Institute of Organic Chemistry, Chinese Academy of Sciences, 354 Fenglin Lu, Shanghai 200032, People's Republic of China, and National Institute of Advanced Industrial Science and Technology (AIST), 1-8-31 Midorigaoka, Ikeda, Osaka 563-8577, Japan

Received July 26, 2004

The reactions of the COT-coordinated diiron cationic bridging carbyne complexes $[\text{Fe}_2(\mu\text{-CAr})(\text{CO})_4(\eta^8\text{-C}_8\text{H}_8)]\text{BF}_4$ (**1**, Ar = C₆H₅; **2**, Ar = *p*-CH₃C₆H₄; **3**, Ar = *p*-CF₃C₆H₄) with *p*-methylaniline gave the COT-coordinated diiron Fischer-type carbene complexes $[\text{Fe}_2\{=\text{C}(\text{Ar})\text{NHC}_6\text{H}_4\text{CH}_3\text{-}p\}(\mu\text{-CO})(\text{CO})_3(\eta^8\text{-C}_8\text{H}_8)]$ (**7**, Ar = C₆H₅; **8**, Ar = *p*-CH₃C₆H₄; **9**, Ar = *p*-CF₃C₆H₄). Heating the solution of diiron carbene complexes $[\text{Fe}_2\{=\text{C}(\text{Ar})\text{NHC}_6\text{H}_5\}(\mu\text{-CO})(\text{CO})_3(\eta^8\text{-C}_8\text{H}_8)]$ (**4**, Ar = C₆H₅; **5**, Ar = *p*-CH₃C₆H₄; **6**, Ar = *p*-CF₃C₆H₄) in benzene in a sealed tube at 85–90 °C for 72 h afforded the chelated diiron carbene complex $[\text{Fe}_2\{=\text{C}(\text{C}_6\text{H}_5)\text{-NC}_6\text{H}_5\}(\eta^2:\eta^3:\eta^2\text{-C}_8\text{H}_9)(\text{CO})_4]$ (**4a**), C₈ ring addition products $[\text{Fe}_2\{\text{N}(\text{C}_6\text{H}_5)=\text{C}(\text{Ar})(\eta^1:\eta^3:\eta^2\text{-C}_8\text{H}_9)\}(\text{CO})_5]$ (**10**, Ar = C₆H₅; **12**, Ar = *p*-CH₃C₆H₄; **14**, Ar = *p*-CF₃C₆H₄), and C₇ contraction ring products $[\text{Fe}_2\{\text{N}(\text{C}_6\text{H}_5)=\text{C}(\text{Ar})\text{CH}(\eta^2:\eta^3\text{-C}_7\text{H}_8)\}(\text{CO})_4]$ (**11**, Ar = C₆H₅; **13**, Ar = *p*-CH₃C₆H₄; **15**, Ar = *p*-CF₃C₆H₄), respectively. The similar thermolysis of complexes **7** and **8** afforded corresponding thermolysis products $[\text{Fe}_2\{=\text{C}(\text{C}_6\text{H}_5)\text{NC}_6\text{H}_4\text{CH}_3\text{-}p\}(\eta^2:\eta^3:\eta^2\text{-C}_8\text{H}_9)(\text{CO})_4]$ (**7a**), $[\text{Fe}_2\{\text{N}(\text{C}_6\text{H}_4\text{CH}_3\text{-}p)=\text{C}(\text{Ar})(\eta^1:\eta^2:\eta^3\text{-C}_8\text{H}_9)\}(\text{CO})_5]$ (**16**, Ar = C₆H₅; **18**, Ar = *p*-CH₃C₆H₄), and $[\text{Fe}_2\{\text{N}(\text{C}_6\text{H}_4\text{CH}_3\text{-}p)=\text{C}(\text{Ar})\text{CH}(\eta^2:\eta^3\text{-C}_7\text{H}_8)\}(\text{CO})_4]$ (**17**, Ar = C₆H₅; **19**, Ar = *p*-CH₃C₆H₄), respectively. Interestingly, products **4a** and **7a** were transformed into the eight-membered ring products **10** and **16** and seven-membered ring products **11** and **17**, respectively, under similar conditions. Surprisingly, compounds **10**, **16**, and **18** can also be partially transformed into compounds **11**, **17**, and **19**, respectively, by further thermolysis at higher temperature (100–105 °C). The structures of complexes **7**, **10**, **11**, **18**, and **19** have been established by X-ray diffraction studies.

Introduction

Our interest in the synthesis, structure, and chemistry of alkene-metal carbene and carbyne complexes stems from the possible involvement of these species in some reactions catalyzed by organometallic compounds.^{1,2} In recent years, olefin-coordinated transition-metal carbene and carbyne complexes, as a part of a broader investigation of transition-metal carbene and carbyne complexes, have been examined extensively, and a considerable number of olefin-coordinated dimetal bridging carbene and bridging carbyne complexes have been synthesized in our laboratory.^{3–5} However, the olefin-coordinated dimetallic Fischer-type carbene or carbyne complexes are rare.^{5a,c,6} Recently, in the course of our

study on the cyclooctatetraene (COT)-coordinated diiron bridging carbene and bridging carbyne complexes, we found that the COT ligand in diiron cationic bridging carbyne complexes $[\text{Fe}_2(\mu\text{-CAr})(\text{CO})_4(\eta^8\text{-C}_8\text{H}_8)]\text{BF}_4$ are activated toward attack by nucleophiles, leading to nucleophilic addition or breaking of the COT ring, the first example of such an activation of an olefin by a diiron bridging carbyne moiety,^{5a} and we have obtained a new type of the COT-coordinated diiron Fischer-type carbene complexes $[\text{Fe}_2\{=\text{C}(\text{Ar})\text{NHC}_6\text{H}_5\}(\mu\text{-CO})(\text{CO})_3(\eta^8\text{-C}_8\text{H}_8)]$ (**4**, Ar = C₆H₅; **5**, Ar = *p*-CH₃C₆H₄; **6**, Ar = *p*-CF₃C₆H₄) from the reactions of the COT-coordinated diiron cationic bridging carbyne complexes $[\text{Fe}_2(\mu\text{-CAr})(\text{CO})_4(\eta^8\text{-C}_8\text{H}_8)]\text{BF}_4$ (**1**, Ar = C₆H₅; **2**, Ar = *p*-CH₃C₆H₄; **3**, Ar = *p*-CF₃C₆H₄) with aniline (eq 1).^{5b,c}

It is known that the chemistry of dimetallic Fischer-type carbene complexes has drawn an enormous interest due to their novel stoichiometric or catalytic reactivity in organic synthesis⁷ and that the olefin ligands in transition-metal complexes exhibit high reactivities.⁸

[†] Dedicated to Prof. Lixin Dai on the occasion of his 80th birthday and in recognition of his brilliant contributions to organic and organometallic chemistry.

[‡] Shanghai Institute of Organic Chemistry.

[§] National Institute of Advanced Industrial Science and Technology.

(1) Suess-Fink, G.; Meister, G. *Adv. Organomet. Chem.* **1993**, *35*, 41.

(2) (a) Gladfelter, W. L.; Roessel, K. J. In *The Chemistry of Metal Cluster Complexes*; Shriver, D. F., Kaesz, H. D., Adams, R. D., Eds.; VCH: Weinheim, Germany, 1990; p 392. (b) Maire, G. In *Metal Clusters in Catalysis*; Gates, B. C., Guzzi, L., Knoezinger, H., Eds.; Elsevier: Amsterdam, The Netherlands, 1986; p 509. (c) Dickson, R. S.; Greaves, B. C. *Organometallics* **1993**, *12*, 3249.

(3) Chen, J.-B.; Li, D.-S.; Yu, Y.; Jin, Z.-S.; Zhou, Q.-L.; Wei, G.-C. *Organometallics* **1993**, *12*, 3885.

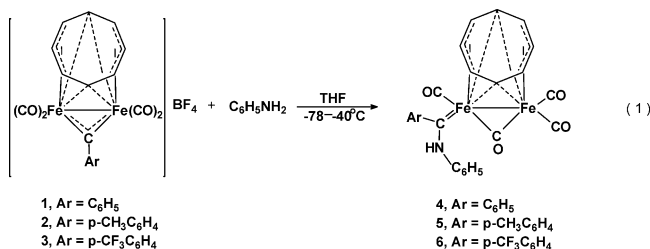
(4) Yu, Y.; Chen, J.-B. *Organometallics* **1993**, *12*, 4731.

(5) (a) Zhang, S.; Xu, Q.; Sun, J.; Chen, J.-B. *Organometallics* **2002**, *21*, 4572. (b) Zhang, S.; Xu, Q.; Sun, J.; Chen, J.-B. *Organometallics* **2003**, *22*, 1816. (c) Zhang, S.; Xu, Q.; Sun, J.; Chen, J.-B. *Chem. Eur. J.* **2003**, *9*, 5111.

(6) Yu, Y.; Sun, J.; Chen, J.-B. *J. Organomet. Chem.* **1997**, *533*, 13.

(7) For review, see: M. A. Sierra, *Chem. Rev.* **2000**, *100*, 3591.

(8) Limanto, J.; Tallarico, J. A.; Porter, J. R.; Khuong, K. S.; Houk, K. N.; Snapper, M. L. *J. Am. Chem. Soc.* **2002**, *124*, 14748.



However, only very little is known^{5b,c} about the reactivity of the olefin-coordinated dimetallic Fischer-type carbene complexes. We are now interested in examining the reactivity of the olefin-coordinated dimetallic Fischer-type carbene complexes.

To further explore the effect of different primary amines on the reactivity of the COT-coordinated diiron cationic bridging carbene complexes and resulting products and to compare the thermolysis reactivity of the COT-coordinated diiron Fischer-type carbene complexes with monometallic Fischer-type carbene complexes, we synthesized the diiron carbene complexes with an aryl(methylanilino)carbene ligand, [Fe₂{=C(Ar)NHC₆H₄-CH₃-*p*}(μ-CO)(CO)₃(η⁸-C₈H₈)] (**7**, Ar = C₆H₅; **8**, Ar = *p*-CH₃C₆H₄; **9**, Ar = *p*-CF₃C₆H₄), from cationic bridging carbene complexes **1–3** and *p*-methylaniline and examined their thermolysis reactions. In this paper we report the syntheses of complexes **7–9** and the remarkable thermolysis reactions of these complexes involving analogous complexes **4–6**.

Experimental Section

All procedures were performed under a dry, oxygen-free N₂ atmosphere by using standard Schlenk techniques. All solvents employed were reagent grade and dried by refluxing over appropriate drying agents and stored over 4 Å molecular sieves under N₂ atmosphere. Tetrahydrofuran and diethyl ether were distilled from sodium benzophenone ketyl, while petroleum ether (30–60 °C) and CH₂Cl₂ were distilled from CaH₂. The neutral alumina (Al₂O₃, 100–200 mesh) used for chromatography was deoxygenated at room temperature under high vacuum for 16 h, deactivated with 5% w/w N₂-saturated water, and stored under N₂ atmosphere. Compounds *p*-CH₃C₆H₄NH₂, aniline-*d*₇, and benzene-*d*₆ were purchased from Aldrich Chemical Co. or Acros Organics Co. Diiron cationic bridging carbene complexes [Fe₂(μ-CAr)(CO)₄(η⁸-C₈H₈)]BF₄ (**1**, Ar = C₆H₅; **2**, Ar = *p*-CH₃C₆H₄; **3**, Ar = *p*-CF₃C₆H₄) and diiron carbene complexes [Fe₂{=C(Ar)NHC₆H₅}(μ-CO)(CO)₃(η⁸-C₈H₈)] (**4**, Ar = C₆H₅; **5**, Ar = *p*-CH₃C₆H₄; **6**, Ar = *p*-CF₃C₆H₄) were prepared as previously described.^{5b,c}

The IR spectra were measured on a Perkin-Elmer 983G spectrophotometer. All ¹H NMR and ¹³C NMR spectra were recorded at ambient temperature in acetone-*d*₆ with TMS as the internal reference using a Bruker AM-300 spectrometer. Electron ionization mass spectra (EIMS) were run on a Hewlett-Packard 5989A spectrometer. Melting points obtained on samples in sealed nitrogen-filled capillaries are uncorrected.

Reaction of [Fe₂(μ-CC₆H₅)(η⁸-C₈H₈)(CO)₄]BF₄ (1**) with *p*-CH₃C₆H₄NH₂ to Give [Fe₂{=C(C₆H₅)NHC₆H₄CH₃-*p*}(μ-CO)(CO)₃(η⁸-C₈H₈)] (**7**).** To freshly prepared **1** (0.253 g, 0.54 μmol) dissolved in 50 mL of THF at -78 °C was added *p*-CH₃C₆H₄NH₂ (0.115 g, 1.09 mmol). After stirring at -78 to -40 °C for 3–4 h, the resulting solution was evaporated under high vacuum at -40 °C to dryness. The dark red residue was chromatographed on Al₂O₃ at -25 °C with petroleum ether/CH₂Cl₂ (10:2) as the eluant. The brown-red band was eluted and collected. After vacuum removal of the solvent, the crude product was recrystallized from petroleum ether/CH₂Cl₂ at -80

°C to give 0.160 g (71%, based on **1**) of purple-red crystals of **7**: mp 80–82 °C dec; IR (CH₂Cl₂) ν(CO) 1987 (vs), 1965 (m), 1931 (s), 1694 (w) cm⁻¹; ¹H NMR (CD₃COCD₃) δ 11.36 (s, 1H, NH), 7.32–6.75 (m, 9H, C₆H₅ + *p*-CH₃C₆H₄), 4.38 (s, 8H, C₈H₈), 2.21 (s, 3H, *p*-CH₃C₆H₄); MS *m/e* 467 (M⁺ - 2CO), 439 (M⁺ - 3CO), 411 [M⁺ - Fe(CO)₂], 383 [M⁺ - Fe(CO)₃], 355 [M⁺ - Fe₂(CO)₂]. Anal. Calcd for C₂₆H₂₁O₄NFe₂: C, 59.70; H, 4.04; N, 2.67. Found: C, 59.35; H, 4.10; N, 2.81.

Reaction of [Fe₂(μ-CC₆H₄CH₃-*p*)(η⁸-C₈H₈)(CO)₄]BF₄ (2**) with *p*-CH₃C₆H₄NH₂ to Give [Fe₂{=C(C₆H₄CH₃-*p*)NHC₆H₄CH₃-*p*}(μ-CO)(CO)₃(η⁸-C₈H₈)] (**8**).** Freshly prepared **2** (0.238 g, 0.49 mmol) in 50 mL of THF was treated, as described for the reaction of **1** with *p*-CH₃C₆H₄NH₂, with 0.105 g (1.00 mmol) of *p*-CH₃C₆H₄NH₂ at -78 to -40 °C for 3 h. Further treatment of the resulting solution as described above afforded 0.142 g (53%, based on **2**) of purple-red crystalline **8**: mp 64–66 °C dec; IR (CH₂Cl₂) ν(CO) 1986 (vs), 1966 (m), 1929 (s), 1693 (w) cm⁻¹; ¹H NMR (CD₃COCD₃) δ 11.36 (s, 1H, NH), 7.12–6.76 (m, 8H, 2 *p*-CH₃C₆H₄), 4.37 (s, 8H, C₈H₈), 2.29 (s, 3H, *p*-CH₃C₆H₄), 2.22 (s, 3H, *p*-CH₃C₆H₄); MS *m/e* 509 (M⁺ - CO), 481 (M⁺ - 2CO), 453 (M⁺ - 3CO), 425 [M⁺ - Fe(CO)₂], 397 [M⁺ - Fe(CO)₃], 369 [M⁺ - Fe₂(CO)₂]. Anal. Calcd for C₂₇H₂₃O₄NFe₂: C, 58.14; H, 4.31; N, 2.61. Found: C, 58.44; H, 4.35; N, 2.76.

Reaction of [Fe₂(μ-CC₆H₄CF₃-*p*)(η⁸-C₈H₈)(CO)₄]BF₄ (3**) with *p*-CH₃C₆H₄NH₂ to Give [Fe₂{=C(C₆H₄CF₃-*p*)NHC₆H₄CH₃-*p*}(μ-CO)(CO)₃(η⁸-C₈H₈)] (**9**).** As described for the reaction of **1** with *p*-CH₃C₆H₄NH₂, freshly prepared **3** (0.253 g, 0.47 mmol) was treated with *p*-CH₃C₆H₄NH₂ (0.100 g, 0.95 mmol) in THF at -78 to -40 °C for 3 h. Further treatment of the resulting solution as described in the reaction of **1** with *p*-CH₃C₆H₄NH₂ gave 0.091 g (32%, based on **3**) of **9** as purple-red crystals: mp 90–92 °C dec; IR (CH₂Cl₂) ν(CO) 1988 (vs), 1968 (m), 1933 (s), 1705 (w) cm⁻¹; ¹H NMR (CD₃COCD₃) δ 11.34 (s, 1H, NH), 7.63–6.82 (m, 8H, *p*-CH₃C₆H₄ + *p*-CF₃C₆H₄), 4.40 (s, 8H, C₈H₈), 2.21 (s, 3H, *p*-CH₃C₆H₄); MS *m/e* 563 (M⁺ - CO), 535 (M⁺ - 2CO), 507 (M⁺ - 3CO), 479 [M⁺ - Fe(CO)₂]. Anal. Calcd for C₂₇H₂₀O₄F₃NFe₂: C, 52.83; H, 3.41; N, 2.37. Found: C, 52.52; H, 3.70; N, 1.99.

Reaction of **1 with C₆D₅ND₂ to Give [Fe₂{=C(C₆H₅)NDC₆D₅}(μ-CO)(CO)₃(η⁸-C₈H₈)] (**4-d₆**).** To 0.150 g (0.30 mmol) of freshly prepared **1** dissolved in 50 mL of THF at -78 °C was added 0.070 mL (0.80 mmol) of C₆D₅ND₂. After stirring at -78 to -40 °C for 3 h, the resulting solution was evaporated under high vacuum at -40 °C to dryness, and the dark red residue was extracted with petroleum ether/CH₂Cl₂ (10:1). The red extracted solution was evaporated in vacuo at -40 °C to dryness, and the residue was recrystallized from petroleum ether/CH₂Cl₂ at -80 °C to give 0.280 g (89%, based on **1**) of deep red crystals of **4-d₆**: mp 144–146 °C dec; IR (CH₂Cl₂) ν(CO) 1987 (s), 1931 (vs), 1697 (m, br) cm⁻¹; ¹H NMR (CD₃COCD₃) δ 7.26–6.92 (m, 5H, C₆H₅), 4.39 (s, 8H, C₈H₈), 11.37 (br, 0.2H, C₆H₅NH). The appearance of a weak signal at δ 11.37 is indicative of the existence of a little N-undeuterated compound [Fe₂{=C(C₆H₅)NHC₆D₅}(μ-CO)(CO)₃(η⁸-C₈H₈)] in the product.

Thermolysis of **4 to Give [Fe₂{=C(C₆H₅)NC₆H₅}(η²:η³:η²-C₈H₉)(CO)₄] (**4a**), [Fe₂{N(C₆H₅)=C(C₆H₅)(η¹:η²:η³-C₈H₉)}(CO)₅] (**10**), and [Fe₂{N(C₆H₅)=C(C₆H₅)CH(η²:η³-C₇H₉)}(CO)₄] (**11**).** Compound **4** (0.100 g, 0.20 mmol) was dissolved in benzene (20 mL) in a quartz tube. The tube was cooled at -80 °C to freeze the benzene solution and sealed under high vacuum. The sealed tube was heated to 85–90 °C for 72 h. After cooling, the dark red solution was evaporated in vacuo to dryness. The residue was chromatographed on Al₂O₃ with petroleum ether as the eluant. The magenta band which eluted first was collected, then a brown band was eluted with petroleum ether/CH₂Cl₂ (10:1). A third brown-red band was eluted with petroleum ether/CH₂Cl₂/Et₂O (10:2:1). After vacuum removal of the solvent from the above three eluates, the residues were recrystallized from petroleum ether or petroleum

ether/CH₂Cl₂ at -80 °C. From the first fraction, 0.010 g (10%) of purple-red crystals of **11** was obtained: mp 120–122 °C; IR (CH₂Cl₂) ν (CO) 1999 (m), 1967 (s), 1930 (m), 1912 (w) cm⁻¹; ¹H NMR (CD₃COCD₃) δ 7.51–7.02 (m, 10H; C₆H₅), 5.44 (t, 1H, *J* = 6.2 Hz, CH), 5.13 (m, 2H, CH), 3.50 (m, 2H, CH), 2.34 (m, 1H, CH), 1.86 (m, 1H, CH₂), 1.63 (t, 1H, *J* = 8.0 Hz, CH), 1.47 (d, 1H, *J* = 12.7 Hz, CH₂); ¹³C NMR (CD₃COCD₃) δ 219.4, 212.6, 202.5 (CO), 158.8, 139.7, 132.6, 129.5, 129.3, 128.7, 127.9, 126.1, 125.3, 117.5 (Ar-C), 88.9, 84.9, 64.5, 64.2, 58.9, 46.3, 44.7, 39.8 (C₈H₉); MS *m/e* 509 (M⁺), 481 (M⁺ - CO), 453 (M⁺ - 2CO), 425 (M⁺ - 3CO), 397 [M⁺ - Fe(CO)₂], 285 [M⁺ - Fe₂(CO)₄]. Anal. Calcd for C₂₅H₁₉O₄NFe₂: C, 58.98; H, 3.76; N, 2.75. Found: C, 59.58; H, 4.01; N, 2.67. From the second deep red fraction, 0.026 g (25%) of deep red crystalline **4a**^{5b} was obtained: mp 178–180 °C dec; IR (CH₂Cl₂) ν (CO) 1999 (m), 1964 (s), 1934 (m) cm⁻¹; ¹H NMR (CD₃COCD₃) δ 7.21–6.50 (m, 10H, C₆H₅), 4.44 (t, 1H, *J* = 6.3 Hz, CH), 4.07 (t, 1H, *J* = 6.8 Hz, CH), 3.62 (dd, 1H, *J* = 15.4, 8.4 Hz, CH), 3.43 (t, 1H, *J* = 6.5 Hz, CH), 3.37 (t, 1H, *J* = 6.9 Hz, CH), 3.02 (dd, 1H, *J* = 8.7, 6.0 Hz, CH), 2.76 (m, 1H, CH₂), 2.61 (dd, 1H, *J* = 13.5, 7.5 Hz, CH), 1.62 (m, 1H, CH₂); ¹³C NMR (CD₃COCD₃) δ 235.6 (C_{carbene}), 217.7, 217.1, 216.5, 215.5 (CO), 158.3, 150.8, 128.9, 128.2, 126.8, 125.1, 124.1, 123.5 (Ar-C), 87.6, 80.1, 68.7, 53.9, 52.8, 42.1, 20.7, 19.1 (C₈H₉); MS *m/e* 481 (M⁺ - CO), 453 (M⁺ - 2CO), 425 (M⁺ - 3CO), 397 [M⁺ - Fe(CO)₂]. Anal. Calcd for C₂₅H₁₉O₄NFe₂: C, 58.98; H, 3.76; N, 2.75. Found: C, 58.78; H, 3.92; N, 2.82. From the third brown-red fraction, 0.055 g (52%) of brown-red crystalline **10** was obtained: mp >200 °C; IR (CH₂Cl₂) ν (CO) 2030 (s), 1966 (vs), 1907 (w) cm⁻¹; ¹H NMR δ 7.31–6.95 (m, 10H, C₆H₅), 5.30 (dd, 1H, *J* = 8.9, 5.2 Hz, CH), 4.78 (t, 1H, *J* = 4.6 Hz, CH), 4.64 (t, 1H, *J* = 7.5 Hz, CH), 4.52 (t, 1H, *J* = 6.5 Hz, CH), 3.77 (t, 1H, *J* = 3.3 Hz, CH), 3.66 (dd, 1H, *J* = 16.3, 7.6 Hz, CH), 2.29 (dt, 1H, *J* = 8.0, 1.5 Hz, CH), 2.13 (dd, 1H, *J* = 16.3, 7.6, 1.3 Hz, CH₂), 1.86 (m, 1H, CH₂); ¹³C NMR (CD₃COCD₃) δ 220.0, 214.2, 207.2 (CO), 160.9, 130.5, 129.6, 129.5, 129.0, 126.4, 122.9 (Ar-C), 88.9, 85.1, 81.0, 74.5, 71.0, 70.1, 56.5, 38.3, 28.4 (C₈H₉); MS *m/e* 481 (M⁺ - 2CO), 425 [M⁺ - Fe(CO)₂], 397 [M⁺ - Fe(CO)₃]. Anal. Calcd for C₂₆H₁₉O₅NFe₂: C, 58.14; H, 3.57; N, 2.61. Found: C, 57.72; H, 3.72; N, 2.86.

Thermolysis of 4 in Benzene-d₆ to Give 4a, 10, and 11. Using the same procedures above, 0.150 g (0.28 mmol) of **4** in benzene-d₆ in a quartz tube was heated to 85–90 °C for 72 h. The dark resulting solution was worked up as above to afford 0.024 g (23%) of **4a**, 0.052 g (49%) of brown-red crystals of **10**, and 0.011 g (14%) of purple-red crystalline **11**, which were identified by their IR and ¹H NMR spectra.

Thermolysis of 4 in Benzene/D₂O to Give 4a, 10, and 11. With the same procedures described above, 0.150 g (0.28 mmol) of **4** in 15 mL of benzene and 0.50 mL of deuterium oxide (D₂O) in a quartz tube were heated to 85–90 °C for 72 h. The dark resulting solution was worked up as described above to afford 0.018 g (17%) of **4a**, 0.052 g (39%) of brown-red crystals of **10**, and 0.008 g (10%) of purple-red crystalline **11**, which were identified by their IR and ¹H NMR spectra.

Thermolysis of 4-d₆ to Give [Fe₂{=C(C₆H₅)NC₆D₅}(η^2 : η^3 : η^2 -C₈H₈D)(CO)₄] (4a-d₆), [Fe₂{N(C₆D₅)=C(C₆H₅)(η^1 : η^2 : η^3 -C₈H₈D)}(CO)₅] (10-d₆), and [Fe₂{N(C₆D₅)=C(C₆H₅)CH(η^2 : η^3 -C₇H₇D)}(CO)₄] (11-d₆). As described for the thermolysis of **4**, compound **4-d₆** (0.050 g, 0.09 mmol) in benzene in a quartz tube was heated to 85–90 °C for 72 h. Subsequent treatment as described for the thermolysis of **4** afforded 0.08 g (24%) of deep red crystalline **4a-d₆**, 0.016 g (47%) of brown-red crystals of **10-d₆**, and 0.004 g (10%) of **11-d₆** as purple-red crystals. **4a-d₆**: mp 126–128 °C dec; IR (CH₂Cl₂) ν (CO) 1997 (m), 1963 (s), 1934 (m) cm⁻¹; ¹H NMR (CD₃COCD₃) δ 7.09–6.56 (m, 5H, C₆H₅), 4.43 (t, 1H, *J* = 6.3 Hz, CH), 4.06 (t, 1H, *J* = 6.8 Hz, CH), 3.61 (dd, 1H, *J* = 15.4, 8.4 Hz, CH), 3.42 (t, 1H, *J* = 6.5 Hz, CH), 3.37 (t, 1H, *J* = 6.9 Hz, CH), 3.02 (dd, 1H, *J* = 8.7, 6.0 Hz, CH), 2.76 (m, 0.2H, CH₂), 2.61 (dd, 1H, *J* = 13.5, 7.5 Hz, CH), 1.60 (m, 1H, CH₂). **10-d₆**: mp 156–158 °C; IR (CH₂-

Cl₂) ν (CO) 2030 (s), 1966 (vs), 1907 (w) cm⁻¹; ¹H NMR δ 7.28 (m, 5H, C₆H₅), 5.31 (dd, 1H, *J* = 8.9, 5.2 Hz, CH), 4.78 (t, 1H, *J* = 4.6 Hz, CH), 4.63 (t, 1H, *J* = 7.5 Hz, CH), 4.52 (t, 1H, *J* = 6.5 Hz, CH), 3.76 (t, 1H, *J* = 3.3 Hz, CH), 3.66 (dd, 1H, *J* = 16.3, 7.6 Hz, CH), 2.29 (dt, 1H, *J* = 8.0, 1.5 Hz, CH), 2.13 (dd, 0.2H, CH₂), 1.86 (m, 1H, CH₂). **11-d₆**: mp 116–118 °C; IR (CH₂-Cl₂) ν (CO) 1999 (m), 1967 (s), 1930 (m), 1912 (w) cm⁻¹; ¹H NMR (CD₃COCD₃) δ 7.50–7.22 (m, 5H; C₆H₅), 5.44 (t, 1H, *J* = 6.2 Hz, CH), 5.11 (m, 2H, CH), 3.49 (m, 2H, CH), 2.33 (m, 1H, CH), 1.86 (m, 0.2H, CH₂), 1.63 (t, 1H, *J* = 8.0 Hz, CH), 1.47 (d, 1H, *J* = 12.7 Hz, CH₂).

Thermolysis of 4a to Give 10 and 11. Using the same procedures as those of the thermolysis of **4**, 0.100 g (0.20 mmol) of **4a** in benzene in a quartz tube was heated to 90 °C for 72 h. The dark resulting solution was worked up as described for the thermolysis of **4** to afford 0.055 g (52%) of brown-red crystals of **10** and 0.011 g (10%) of purple-red crystalline **11**, which were identified by their IR and ¹H NMR spectra.

Thermolysis of 10 to Give 11. As in the thermolysis of **4** above, a solution of compound **10** (0.112 g, 0.21 mmol) in 15 mL of benzene in a quartz tube was heated to 100–105 °C for 72 h. Further treatment of the resulting solution in a manner similar to that described in the thermolysis of **4** gave 0.012 g (11%) of purple-red crystals of **11** and 0.064 g (57%) of unchanged compound **10**, which were identified by their IR and ¹H NMR spectra.

Thermolysis of 5 to Give [Fe₂{N(C₆H₅)=C(C₆H₄CH₃-*p*)-(η^1 : η^2 : η^3 -C₈H₉)}(CO)₅] (12) and [Fe₂{N(C₆H₅)=C(C₆H₄CH₃-*p*)CH(η^2 : η^3 -C₇H₈)}(CO)₄] (13). As described for the thermolysis of **4**, compound **5** (0.300 g, 0.57 mmol) in benzene in a quartz tube was heated to 85–90 °C for 72 h. Subsequent treatment as described for the thermolysis of **4** afforded 0.150 g (47%) of brown-red crystalline **12** and 0.030 g (11%) of **13** as purple-red crystals. **12**: mp >200 °C; IR (CH₂Cl₂) ν (CO) 2029 (s), 1965 (vs), 1906 (w) cm⁻¹; ¹H NMR (CD₃COCD₃) δ 7.28–6.95 (m, 9H, C₆H₅ + *p*-CH₃C₆H₄), 5.64 (s, 1H, CH₂Cl₂), 5.29 (dd, 1H, *J* = 8.6, 5.0 Hz, CH), 4.77 (t, 1H, *J* = 5.5 Hz, CH), 4.63 (t, 1H, *J* = 7.2 Hz, CH), 4.52 (t, 1H, *J* = 6.5 Hz, CH), 3.76 (br, 1H, CH), 3.63 (m, 1H, CH), 2.26 (m, 1H, CH), 2.06 (m, 1H, CH₂), 1.86 (m, 1H, CH₂); ¹³C NMR (CD₃COCD₃) δ 219.9, 214.1, 207.1 (CO), 187.5, 154.4, 140.8, 131.6, 129.6, 129.5, 129.4, 126.3, 122.7 (Ar-C), 88.8, 85.0, 81.0, 74.6, 69.9, 56.4, 37.9, 28.4, 21.1 (C₈H₉ + *p*-CH₃C₆H₄); MS *m/e* 495 (M⁺ - 2CO), 467 (M⁺ - 3CO), 439 (M⁺ - 4CO), 411 [M⁺ - Fe(CO)₃], 84 (CH₂Cl₂). Anal. Calcd for C₂₇H₂₁O₅NFe₂·0.5CH₂Cl₂: C, 55.64; H, 3.74; N, 2.36. Found: C, 55.81; H, 3.73; N, 2.24. **13**: mp 130–132 °C; IR (CH₂Cl₂) ν (CO) 1999 (m), 1966 (s), 1928 (m), 1911 (w) cm⁻¹; ¹H NMR (CD₃COCD₃) δ 7.49–7.01 (m, 9H, C₆H₅ + *p*-CH₃C₆H₄), 5.42 (t, 1H, *J* = 6.4 Hz, CH), 5.10 (m, 2H, CH), 3.51 (m, 2H, CH), 2.32 (m, 1H, CH), 2.26 (s, 3H, CH₃C₆H₄), 1.83 (m, 1H, CH₂), 1.62 (t, 1H, *J* = 8.0 Hz, CH), 1.47 (d, 1H, *J* = 11.9 Hz, CH₂); ¹³C NMR (CD₃COCD₃) δ 219.5, 212.7, 207.2, 202.7 (CO), 159.1, 139.6, 137.1, 135.9, 132.6, 129.5, 129.4, 128.8, 128.7, 126.3, 125.4 (Ar-C), 89.0, 85.1, 64.6, 62.4, 59.1, 46.3, 44.8, 40.0, 21.1 (C₈H₉ + *p*-CH₃C₆H₄); MS *m/e* 523 (M⁺), 495 (M⁺ - CO), 467 (M⁺ - 2CO), 439 (M⁺ - 3CO). Anal. Calcd for C₂₆H₂₁O₄NFe₂: C, 59.69; H, 4.05; N, 2.68. Found: C, 59.58; H, 3.73; N, 2.24.

Thermolysis of 6 to Give [Fe₂{N(C₆H₅)=C(C₆H₄CF₃-*p*)-(η^1 : η^2 : η^3 -C₈H₉)}(CO)₅] (14) and [Fe₂{N(C₆H₅)=C(C₆H₄CF₃-*p*)CH(η^2 : η^3 -C₇H₈)}(CO)₄] (15). Similar to the procedures used in the thermolysis of **4**, compound **6** (0.200 g, 0.35 mmol) in benzene in a quartz tube was heated to 85–90 °C for 72 h. The resulting solution was worked up as described for the thermolysis of **4** to produce 0.080 g (38%) of brown-red crystals of **14** and 0.016 g (8%) of **15** as purple-red crystals. **14**: mp >200 °C; IR (CH₂Cl₂) ν (CO) 2031 (s), 1968 (vs), 1909 (w) cm⁻¹; ¹H NMR (CD₃COCD₃) δ 7.64–6.99 (m, 9H, C₆H₅ + *p*-CF₃C₆H₄), 5.63 (s, 1H, CH₂Cl₂), 5.32 (dd, 1H, *J* = 8.8, 5.3 Hz, CH), 4.80 (t, 1H, *J* = 5.8 Hz, CH), 4.63 (t, 1H, *J* = 8.0 Hz, CH), 4.55 (t, 1H, *J* = 6.2 Hz, CH), 3.78 (t, 1H, *J* = 2.9 Hz, CH), 3.67 (dd,

1H, $J = 16.4, 7.6$ Hz, CH), 2.35 (m, 1H, $J = 7.8, 1.5$ Hz, CH), 2.17 (m, 1H, CH₂), 1.85 (m, 1H, CH₂); ¹³C NMR (CD₃COCD₃) δ 219.7, 213.9, 207.0 (CO), 186.6, 153.7, 138.7, 130.1, 129.6, 126.7, 125.8, 122.6 (Ar-C), 89.0, 84.9, 80.8, 73.9, 70.0, 56.5, 38.6, 28.1 (C₈H₉ + *p*-CF₃C₆H₄). MS *m/e* 605 (M⁺), 549 (M⁺ - 2CO), 521 (M⁺ - 3CO), 493 (M⁺ - 4CO), 84 (CH₂Cl₂⁺). Anal. Calcd for C₂₇H₁₉O₅F₃NFe₂·0.5CH₂Cl₂: C, 51.00; H, 2.96; N, 2.16. Found: C, 51.50; H, 2.99; N, 2.02. **15**: mp 120–122 °C; IR (CH₂Cl₂) ν (CO) 2040 (m), 2003 (m), 1973 (s), 1936 (s) cm⁻¹; ¹H NMR (CD₃COCD₃) δ 7.77–7.05 (m, 9H, C₆H₅ + *p*-CF₃C₆H₄), 5.48 (t, 1H, $J = 5.7$ Hz, CH), 5.17 (m, 2H, CH), 3.52 (m, 2H, CH), 2.36 (m, 1H, CH), 1.87 (m, 1H, CH₂), 1.66 (t, 1H, $J = 7.7$ Hz, CH), 1.49 (d, 1H, $J = 12.7$ Hz, CH₂); ¹³C NMR (CD₃COCD₃) δ 219.1, 212.4, 206.7, 202.3 (CO), 158.3, 133.4, 129.5, 129.3, 128.8, 128.3, 126.0, 125.6, 124.8 (Ar-C), 89.0, 84.9, 64.7, 62.3, 59.0, 46.9, 44.6, 39.7 (C₈H₉ + *p*-CF₃C₆H₄); MS *m/e* 523 (M⁺), 495 (M⁺ - CO), 467 (M⁺ - 2CO), 439 (M⁺ - 3CO). Anal. Calcd for C₂₆H₁₈F₃O₄NFe₂: C, 54.11; H, 3.14; N, 2.43. Found: C, 54.72; H, 3.56; N, 2.78.

Thermolysis of 7 to Give [Fe₂{=C(C₆H₅)NC₆H₄CH₃-*p*}-(η^2 : η^3 : μ^2 -C₈H₉)(CO)₄] (7a), [Fe₂{N(C₆H₄CH₃-*p*)=C(C₆H₅)(η^1 - η^2 : η^3 -C₈H₉)}(CO)₅] (16), and [Fe₂{N(C₆H₄CH₃-*p*)=C(C₆H₅)-CH(η^2 : η^3 -C₇H₈)}(CO)₄] (17). Compound **7** (0.210 g, 0.43 mmol) was dissolved in benzene (20 mL) in a quartz tube. The tube was cooled at -80 °C to freeze the benzene solution and sealed under high vacuum. The sealed tube was heated to 85–90 °C for 72 h. After cooling, the dark red solution was evaporated in vacuo to dryness. The dark residue was chromatographed on Al₂O₃ with petroleum ether as the eluant. The magenta band which eluted first was collected, then an orange-red band was eluted with petroleum ether/CH₂Cl₂/Et₂O (10:2). A third, brown-red band was eluted with petroleum ether/CH₂Cl₂/Et₂O (10:2:1). The solvents were removed from the above three eluates in vacuo, and the crude products were recrystallized from petroleum ether or petroleum ether/CH₂Cl₂ at -80 °C. From the first fraction, 0.022 g (10%) of purple-red crystals of **17** was obtained: mp 164–166 °C; IR (CH₂Cl₂) ν (CO) 1999 (s), 1966 (vs), 1928 (s), 1912 (m) cm⁻¹; ¹H NMR (CD₃COCD₃) δ 7.51–6.90 (m, 9H; C₆H₅ + *p*-CH₃C₆H₄), 5.44 (t, 1H, $J = 11.7$ Hz, CH), 5.13 (m, 2H, CH), 3.50 (m, 2H, CH), 2.34 (m, 1H, CH), 2.25 (s, 3H, CH₃C₆H₄), 1.86 (m, 1H, CH₂), 1.63 (t, 1H, $J = 7.8$ Hz, CH), 1.47 (d, 1H, $J = 6.9$ Hz, CH₂), 1.29–1.09 (m, 8H, CH₃(CH₂)₄CH₃), 0.86 (m, 6H, CH₃(CH₂)₄CH₃); ¹³C NMR (CD₃COCD₃) δ 219.6, 212.6, 207.1, 202.6 (CO), 156.7, 139.9, 136.2, 134.7, 132.7, 129.7, 129.5, 129.4, 129.1, 128.0, 126.0 (Ar-C), 88.9, 84.9, 64.5, 62.2, 59.0, 46.3, 44.8, 39.9, 20.6 (C₈H₉ + *p*-CH₃C₆H₄); MS *m/e* 495 (M⁺ - CO), 467 (M⁺ - 2CO), 439 (M⁺ - 3CO), 411 (M⁺ - 4CO), 86 (C₆H₁₄⁺). Anal. Calcd for C₂₆H₂₁O₄NFe₂·C₆H₁₄: C, 63.08; H, 4.79; N, 2.30. Found: C, 63.52; H, 4.68; N, 2.66. From the second fraction, 0.070 g (33%) of deep red crystals of **7a** was obtained: mp 112–114 °C dec; IR (CH₂Cl₂) ν (CO) 2004 (m), 1971 (vs), 1942 (m) cm⁻¹; ¹H NMR (CD₃COCD₃) δ 7.1–6.40 (m, 9H, C₆H₅ + *p*-CH₃C₆H₄), 4.42 (t, 1H, $J = 12.9$ Hz, CH), 4.06 (t, 1H, $J = 13.8$ Hz, CH), 3.60 (dd, 1H, $J = 15.0$ Hz, 6.6 Hz, CH), 3.39 (m, 1H, CH), 2.99 (dd, 1H, $J = 9.0, 6.0$ Hz, CH), 2.72 (m, 1H, CH₂), 2.60 (dd, 1H, $J = 13.8$ Hz, 8.1 Hz, CH), 2.23 (s, 3H, CH₃C₆H₄), 1.60 (m, 1H, CH₂); ¹³C NMR (CD₃COCD₃) δ 235.6 (C_{carbene}), 218.4, 217.9, 217.2, 216.2 (CO), 156.7, 151.6, 134.7, 129.7, 128.9, 128.5, 127.0, 124.4, 123.6, 123.5, 95.3 (Ar-C), 88.3, 85.9, 84.2, 80.1, 71.0, 69.3, 62.4, 54.4, 53.5, 42.7, 21.3, 20.8, 19.7 (C₈H₉ + *p*-CH₃C₆H₄); MS *m/e* 495 (M⁺ - CO), 411 [M⁺ - Fe(CO)₂], 299 [M⁺ - Fe₂(CO)₄]. Anal. Calcd for C₂₆H₂₁O₄NFe₂: C, 59.69; H, 4.05; N, 2.68. Found: C, 59.49; H, 4.24; N, 2.62. From the third fraction, 0.062 g (28%) of brown-red crystalline **16** was obtained: mp 136–138 °C dec; IR (CH₂Cl₂) ν (CO) 2029 (s), 1966 (vs), 1906 (w) cm⁻¹; ¹H NMR (CD₃COCD₃) δ 7.28–6.84 (m, 9H, C₆H₅ + *p*-CH₃C₆H₄), 5.29 (dd, 1H, $J = 9.0, 5.4$ Hz, CH), 4.775 (t, 1H, $J = 4.2$ Hz, CH), 4.65 (t, 1H, $J = 7.5$ Hz, CH), 4.52 (t, 1H, $J = 6.6$ Hz, CH), 3.75 (t, 1H, $J = 3.6$ Hz, CH), 3.64 (dd, 1H, $J = 16.4, 7.5$ Hz, CH), 2.29 (m, 1H, CH), 2.26 (s, 3H, CH₃C₆H₄),

2.11 (m, 1H, CH₂), 1.84 (m, 1H, CH₂); ¹³C NMR (CD₃COCD₃) δ 220.0, 207.2, 187.6 (CO), 151.9, 135.9, 134.9, 130.4, 130.0, 129.5, 129.0, 122.7 (Ar-C), 88.9, 85.1, 81.0, 74.5, 70.1, 56.4, 38.3, 28.3, 20.8 (C₈H₉ + *p*-CH₃C₆H₄); MS *m/e* 495 (M⁺ - 2CO), 467 (M⁺ - 3CO), 439 (M⁺ - 4CO). Anal. Calcd for C₂₇H₂₁O₅-NFe₂: C, 58.84; H, 3.84; N, 2.54. Found: C, 58.28; H, 3.62; N, 2.38.

Thermolysis of 7a to Give 16 and 17. Using the same procedures as those for the thermolysis of **7**, 0.074 g (0.13 mmol) of **7a** in benzene in a quartz tube was heated to 90 °C for 72 h. The dark resulting solution was worked up as described for the thermolysis of **7** to afford 0.033 g (43%) of brown-red crystals of **16** and 0.007 g (9%) of purple-red crystalline **17**, which were identified by their IR and ¹H NMR spectra.

Thermolysis of 16 to Give 17. Compound **16** (0.070 g, 0.134 mmol) in benzene in a quartz tube was heated, in a manner similar to that described for the thermolysis of **7**, to 100–105 °C for 72 h. After vacuum removal of the solvent, the residue was worked up as described for the thermolysis of **7** to give 0.007 g (9%) of purple red crystals of **17** and 0.040 g (57%) of unchanged compound **16**, which were identified by their IR and ¹H NMR spectra.

Thermolysis of 8 to Give [Fe₂{N(C₆H₄CH₃-*p*)=C(C₆H₄CH₃-*p*)(η^1 : η^2 : η^3 -C₈H₉)}(CO)₅] (18) and [Fe₂{N(C₆H₄CH₃-*p*)=C(C₆H₄CH₃-*p*)CH(η^2 : η^3 -C₇H₈)}(CO)₄] (19). Similar to the procedures used in the thermolysis of **7**, 0.090 g (0.18 mmol) of **8** in benzene in a quartz tube was heated to 85–90 °C for 72 h. The dark resulting solution was worked up as described for the thermolysis of **7** to afford 0.039 g (41%) of brown-red crystalline **18** and 0.007 g (8%) of purple-red crystals. **18**: mp 78–80 °C; IR (CH₂Cl₂) ν (CO) 2029 (s), 1965 (vs), 1906 (w) cm⁻¹; ¹H NMR (CD₃COCD₃) δ 7.19–6.83 (m, 8H, *p*-CH₃C₆H₄), 5.28 (dd, 1H, $J = 5.1, 9.3$ Hz, CH), 4.76 (t, 1H, $J = 6.0$ Hz, CH), 4.62 (t, 1H, $J = 7.5$ Hz, CH), 4.50 (t, 1H, $J = 6.3$ Hz, CH), 3.74 (t, 1H, $J = 3.0$ Hz, CH), 3.64 (dd, 1H, $J = 15.9, 7.5$ Hz, CH), 2.26 (s, 4H, CH₃C₆H₄ + CH), 2.24 (s, 3H, *p*-CH₃C₆H₄), 2.06 (m, 1H, CH₂), 1.83 (m, 1H, CH₂). ¹³C NMR (CD₃COCD₃) δ 220.0, 207.1, 187.4 (CO), 152.1, 140.7, 135.8, 131.8, 130.0, 129.7, 129.6, 129.5, 122.6 (Ar-C), 88.8, 85.1, 81.0, 74.7, 70.0, 56.4, 38.0, 28.4, 21.2, 20.2 (C₈H₉ + *p*-CH₃C₆H₄); MS *m/e* 453 [M⁺ - Fe(CO)₂], 425 [M⁺ - Fe(CO)₃]. Anal. Calcd for C₂₈H₂₃O₅NFe₂: C, 59.50; H, 4.10; N, 2.48. Found: C, 59.80; H, 4.49; N, 2.21. **19**: mp 164–166 °C; IR (CH₂Cl₂) ν (CO) 1998 (s), 1965 (vs), 1928 (s), 1911 (m) cm⁻¹; ¹H NMR (CD₃COCD₃) δ 7.39–6.91 (m, 8H, 2 *p*-CH₃C₆H₄), 5.40 (t, 1H, $J = 6.3$ Hz, CH), 5.08 (m, 2H, CH), 3.49–3.37 (m, 2H, CH), 2.30 (m, 1H, CH), 2.27 (s, 3H, *p*-CH₃C₆H₄), 2.26 (s, 3H, CH₃C₆H₄), 1.83 (m, 1H, CH₂), 1.61 (t, 1H, $J = 7.8$ Hz, CH), 1.45 (d, 1H, $J = 6.3$ Hz, CH₂), 1.29–1.09 (m, 4H, CH₃(CH₂)₄-CH₃), 0.86 (m, 3H, CH₃(CH₂)₄CH₃); ¹³C NMR (CD₃COCD₃) δ 218.9, 212.2, 206.5, 202.0 (CO); 156.2, 138.9, 136.5, 135.4, 134.0, 132.0, 129.1, 128.8, 128.5, 128.0, 125.4 (Ar-C); 88.2, 84.4, 63.8, 61.6, 58.3, 45.5, 44.2, 39.3, 20.5, 20.0 (C₈H₉ + *p*-CH₃C₆H₄), 25.7, 22.2, 14.9 (C₆H₁₄); MS *m/e* 537 (M⁺), 509 (M⁺ - CO), 481 (M⁺ - 2CO), 426 [M⁺ - Fe(CO)₂], 86 (C₆H₁₄⁺). Anal. Calcd for C₂₇H₂₃O₄NFe₂·0.5C₆H₁₄: C, 62.10; H, 5.21; N, 2.41. Found: C, 62.23; H, 5.24; N, 2.32.

Thermolysis of 18 to Give 19. As described above for the thermolysis of **7**, compound **18** (0.070 g, 0.12 mmol) in benzene in a quartz tube was heated to 100–105 °C for 72 h. After the solvent was evaporated, further treatment of the residue in a manner similar to that described for the thermolysis of **7** gave 0.007 g (10%) of purple-red crystals of **19** and 0.045 g (64%) of unchanged compound **18**, which were identified by their IR and ¹H NMR spectra.

X-ray Crystal Structure Determinations of Complexes 7, 10, 11, 18, and 19. The single crystals of complexes **7**, **10**, **11**, **18**, and **19** suitable for X-ray diffraction study were obtained by recrystallization from petroleum ether/CH₂Cl₂ or petroleum ether/Et₂O at -80 °C. Single crystals were mounted on a glass fiber and sealed with epoxy glue. The X-ray

Table 1. Crystal Data and Experimental Details for Complexes 7, 10, 11, 18, and 19

	7	10	11	18·Et ₂ O	19·CH ₂ Cl ₂
formula	C ₂₆ H ₂₁ O ₄ NFe ₂	C ₂₆ H ₁₉ O ₃ NFe ₂	C ₂₅ H ₁₉ O ₄ NFe ₂	C ₆₀ H ₅₆ O ₁₁ N ₂ Fe ₄	C ₂₈ H ₂₅ O ₄ Cl ₂ NFe ₂
fw	523.14	537.12	509.11	1204.47	622.09
space group	<i>P</i> 1 (No. 2)	<i>P</i> 2 ₁ / <i>n</i> (No. 14)	<i>P</i> 1 (No. 2)	<i>P</i> 2 ₁ / <i>c</i> (No. 14)	<i>P</i> bca (No. 61)
<i>a</i> (Å)	8.2205(8)	7.6928(8)	11.861(13)	17.4782(10)	10.4699(10)
<i>b</i> (Å)	11.1668(10)	23.428(2)	13.882(15)	13.3877(7)	23.469(2)
<i>c</i> (Å)	14.1767(13)	13.1081(13)	14.882(15)	25.9087(15)	23.670(2)
α (deg)	105.139(2)		105.426(19)		90
β (deg)	97.409(2)	103.787(2)	113.33(2)	100.3530(10)	90
γ (deg)	110.053(2)		93.96(2)		90
<i>V</i> (Å ³)	1145.28(18)	2294.3(4)	2126(4)	5963.8(6)	5816.1(10)
<i>Z</i>	2	4	4	4	8
<i>D</i> _{calcd} (g/cm ³)	1.517	1.555	1.590	1.341	1.421
<i>F</i> (000)	536	1096	1040	2488	2544
μ(Mo Kα) (cm ⁻¹)	13.00	13.03	13.97	10.12	12.14
radiation (monochromated in incident beam)	Mo Kα (λ = 0.71073 Å)	MoKα (λ = 0.71073 Å)	Mo Kα (λ = 0.71073 Å)	Mo Kα (λ = 0.71073 Å)	Mo Kα (λ = 0.71073 Å)
diffractometer	Bruker Smart	Bruker Smart	Bruker Smart	Bruker Smart	Bruker Smart
temperature (°C)	20	20	20	20	20
orientation reflns: range (2θ) (deg)	5.561–52.770	4.725–45.108	4.707–36.464	4.334–36.978	4.594–34.888
scan method	ω–2θ	ω–2θ	ω–2θ	ω–2θ	ω–2θ
data collected range, 2θ (deg)	3.06–54.00	3.48–55.10	3.10–50.00	3.44–54.00	3.44–51.10
no. of unique data, total	4868	5122	7345	12935	5423
with <i>I</i> > 2.00σ(<i>I</i>)	3675	3081	2795	4228	2488
no. of params refined	327	383	629	698	325
correct. factors, max.–min.	0.75216–1.00000	0.54902–1.00000	0.42158–1.00000	0.85892–1.00000	0.83686–1.00000
<i>R</i> ^a	0.0386	0.0454	0.1111	0.0737	0.0741
<i>R</i> _w ^b	0.0904	0.0749	0.2482	0.1765	0.1653
quality of fit indicator ^c	0.952	0.827	0.892	0.879	0.944
max. shift/esd. final cycle	0.001	0.002	0.092	0.092	0.091
largest peak (e ⁻ /Å ³)	0.512	0.434	1.501	0.967	0.433
minimum peak (e ⁻ /Å ³)	-0.290	-0.257	-0.898	-0.386	-0.537

^a $R = \sum ||F_o| - |F_c|| / \sum |F_o|$. ^b $R_w = [\sum w(|F_o| - |F_c|)^2 / \sum w|F_o|^2]^{1/2}$; $w = 1/\sigma^2(|F_o|)$. ^c Quality-of-fit = $[\sum w(|F_o| - |F_c|)^2 / (N_{obs} - N_{parameters})]^{1/2}$.

diffraction intensity data for **7**, **10**, **11**, **18**, and **19** were collected with a Bruker Smart diffractometer at 20 °C using Mo Kα radiation with an ω–2θ scan mode.

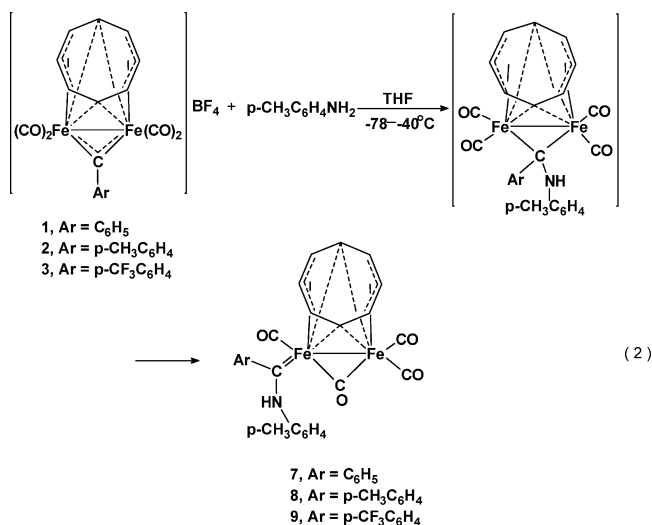
The structures of **7**, **10**, **11**, **18**, and **19** were solved by the direct methods and expanded using Fourier techniques. For the six complexes, the non-hydrogen atoms were refined anisotropically and the hydrogen atoms were included but not refined. The absorption corrections were applied using SADABS. The final cycle of full-matrix least-squares refinement was based on the observed reflections and the variable parameters and converged with unweighted and weighted agreement to give agreement factors of *R* = 0.0386 and *R*_w = 0.0904 for **7**, *R* = 0.0454 and *R*_w = 0.0749 for **10**, *R* = 0.1111 and *R*_w = 0.2482 for **11**, *R* = 0.0737 and *R*_w = 0.1765 for **18**, and *R* = 0.0741 and *R*_w = 0.1653 for **19**. For complex **11**, the *R* factor is relatively high since single crystals suitable for X-ray diffraction were very difficult to obtain and the intensity data were collected at 20 °C. The reflection intensity was evidently decayed during the collection.

The details of the crystallographic data and the procedures used for data collection and reduction information for **7**, **10**, **11**, **18**, and **19** are given in Table 1. The selected bond lengths and angles are listed in Table 2. The atomic coordinates and *B*_{iso}/*B*_{eq}, anisotropic displacement parameters, complete bond lengths and angles, and least-squares planes for **7**, **10**, **11**, **18**, and **19** are given in the Supporting Information. The molecular structures of **7**, **10**, **11**, **18**, and **19** are given in Figures 1–5, respectively.

Results and Discussion

By analogy with the preparation of the COT-coordinated diiron carbene complexes [Fe₂{=C(Ar)NHC₆H₅}-(*μ*-CO)(CO)₃(η⁸-C₈H₈)] (**4**, Ar = C₆H₅; **5**, Ar = *p*-CH₃C₆H₄; **6**, Ar = *p*-CF₃C₆H₄),^{5b,c} freshly prepared (in situ) diiron cationic bridging carbene complexes **1–3** react with *p*-methylaniline in THF at -78 to -40 °C for 3–4 h.

After workup as described in the Experimental Section, the purple-red diiron carbene complexes [Fe₂{=C(Ar)-NHC₆H₄CH₃-*p*}(*μ*-CO)(CO)₃(η⁸-C₈H₈)] (**7**, Ar = C₆H₅; **8**, Ar = *p*-CH₃C₆H₄; **9**, Ar = *p*-CF₃C₆H₄) (eq 2) were obtained in 32–71% isolated yields.



Complexes **7–9** were readily soluble in polar organic solvents but slightly soluble in nonpolar solvents. They are very sensitive to air and temperature in solution and in the solid state. The formulas shown in eq 2 for the three complexes were established by microanalytical data and IR, ¹H NMR, and mass spectra, as well as X-ray crystallography. The IR spectra of complexes **7–9** showed a CO absorption band, characteristic for a bridging CO ligand, at 1693–1705 cm⁻¹ in the ν(CO) region in addition to the three terminal CO absorption

Table 2. Selected Bond Lengths (Å) and Angles (deg) for Complexes 7, 10, 11, 18, and 19^a

	7	10	11	18	19
Fe(1)–Fe(2)	2.7462(5)	2.7599(7)	2.671(4)	2.7626(14)	2.6912(14)
Fe(1)–C(1)	1.913(2)		2.062(14)		2.081(7)
Fe(1)–C(8)	1.916(2)	1.769(4)	1.68(2)	1.748(14)	1.761(9)
Fe(2)–C(8)	1.948(2)				
Fe(1)–C(13)	2.249(3)	2.098(4)	2.378(13)	2.117(8)	2.400(8)
Fe(1)–C(14)	2.121(3)	2.066(4)	2.098(16)	2.058(9)	2.115(8)
Fe(1)–C(15)	2.110(3)	2.162(3)		2.161(8)	
Fe(1)–C(16)	2.182(3)				
Fe(1)–C(19)			2.106(15)		2.114(7)
Fe(2)–C(12)	2.157(4)	2.233(3)	2.034(15)	2.239(7)	2.062(7)
Fe(2)–C(13)			2.477(15)		2.401(8)
Fe(2)–C(16)		2.055(3)		2.060(7)	
Fe(2)–C(17)	2.288(3)		2.089(16)		2.088(7)
Fe(2)–C(18)	2.084(3)		2.030(17)		2.047(7)
Fe(2)–C(19)	2.076(3)			2.239(7)	
Fe(1)–C(9)	1.742(3)	1.784(4)	1.729(17)	1.780(9)	1.763(9)
Fe(2)–C(10)	1.763(3)	1.799(3)	1.724(19)	1.750(9)	1.771(10)
Fe(2)–C(11)	1.751(3)	1.760(4)	1.80(2)	1.795(8)	1.774(8)
C(1)–N(1)	1.328(3)	1.288(3)	1.390(15)	1.282(9)	1.387(8)
Fe(1)–N(1)			1.983(12)		1.994(5)
Fe(2)–N(1)		2.013(2)	1.999(11)	2.041(6)	1.971(5)
C(8)–O(1)	1.187(3)	1.150(4)	1.228(19)	1.157(9)	1.159(8)
C(1)–C(2)	1.487(3)	1.483(4)	1.483(18)	1.444(10)	1.481(9)
C(1)–C(17)		1.493(4)		1.485(10)	
C(1)–C(19)			1.395(19)		1.423(9)
N(1)–C(20)	1.429(3)	1.447(3)	1.459(16)	1.445(8)	1.461(8)
C(12)–C(13)	1.443(6)	1.454(5)	1.47(2)	1.466(9)	1.446(10)
C(13)–C(14)	1.409(7)	1.408(5)	1.38(2)	1.403(10)	1.413(10)
C(14)–C(15)	1.349(6)	1.382(5)	1.47(2)	1.403(10)	1.536(11)
C(15)–C(16)	1.364(7)	1.478(4)	1.54(2)	1.496(9)	1.535(11)
C(16)–C(17)	1.391(6)	1.527(4)	1.50(2)	1.490(11)	1.505(10)
C(16)–C(19)			1.496(19)		1.536(10)
C(17)–C(18)	1.399(5)	1.546(4)	1.43(2)	1.550(10)	1.400(10)
C(18)–C(19)	1.356(5)	1.493(5)		1.500(10)	
C(12)–C(18)			1.39(2)		1.406(10)
C(12)–C(19)	1.426(5)	1.362(5)		1.353(10)	
Fe(1)–C(8)–Fe(2)	90.59(4)				
Fe(1)–Fe(2)–C(8)	44.25(7)				
Fe(2)–Fe(1)–C(8)	45.17(7)	75.51(12)	95.6(6)	77.5(3)	99.4(2)
Fe(2)–Fe(1)–C(1)	129.94(7)		77.2(4)		76.51(19)
Fe(2)–Fe(1)–C(19)	99.10(10)		83.7(5)		83.2(2)
Fe(1)–C(1)–N(1)	122.63(16)		66.8(7)		66.8(3)
Fe(1)–C(1)–C(2)	122.72(16)		125.8(9)		126.8(5)
Fe(1)–Fe(2)–N(1)		148.90(7)	47.6(3)	149.06(18)	47.63(15)
Fe(2)–Fe(1)–N(1)			48.1(3)		46.90(15)
Fe(1)–N(1)–Fe(2)			84.3(4)		85.5(2)
Fe(1)–N(1)–C(1)			73.0(7)		73.5(4)
N(1)–Fe(1)–C(1)			40.1(4)		39.7(2)
Fe(1)–Fe(2)–C(17)	64.86(13)		87.3(5)		87.8(2)
Fe(2)–Fe(1)–C(16)	79.60(15)				
Fe(2)–N(1)–C(1)		115.8(2)	122.9(8)	115.3(5)	125.2(5)
Fe(2)–N(1)–C(20)		123.10(19)	136.3(9)	122.7(5)	114.7(4)
Fe(1)–C(8)–O(1)	135.43(19)	174.1(4)	177.3(16)	175.2(8)	173.2(7)
Fe(2)–C(8)–O(1)	133.88(19)				
N(1)–C(1)–C(2)	114.63(19)	126.2(3)	120.8(11)	125.6(7)	124.0(6)
C(2)–C(1)–C(17)		121.5(3)		122.3(7)	
C(2)–C(1)–C(19)			119.8(13)		118.8(6)
C(1)–N(1)–C(20)	131.97(19)	120.9(3)	118.8(10)	121.8(6)	116.5(5)
C(1)–C(19)–C(16)			131.2(15)		130.9(7)
C(12)–C(13)–C(14)	134.1(4)	125.5(4)	123.7(16)	125.9(7)	128.4(9)
C(13)–C(14)–C(15)	129.6(4)	123.6(3)	125.0(17)	123.3(7)	116.9(8)
C(14)–C(15)–C(16)	128.2(4)	126.1(3)	107.2(12)	126.9(7)	109.5(7)
C(15)–C(16)–C(17)	133.5(5)	116.8(3)	118.1(14)	117.5(7)	116.6(7)
C(16)–C(17)–C(18)	136.8(4)	108.1(3)	125.4(15)	109.5(6)	124.4(7)
C(17)–C(18)–C(19)	128.0(3)	109.9(3)		108.3(6)	
C(17)–C(18)–C(12)			118.7(18)		121.0(7)
C(18)–C(12)–C(13)			128.6(16)		124.5(7)
C(18)–C(19)–C(12)	125.0(3)	126.1(3)		124.8(7)	
C(19)–C(12)–C(13)	133.5(4)	127.0(4)		127.6(7)	
Fe(1)–C–O (av)	177.7	175.8	177.3	176.1	175.9
Fe(2)–C–O (av)	178.3	177.2	176.0	177.7	176.8

^a Estimated standard deviations in the least significant figure are given in parentheses.

bands at 1986–1988, 1965–1968, and 1929–1933 cm⁻¹. The ¹H NMR spectra of **7**–**9** showed a single-line signal for the COT ligand as that of the original eight-membered ring in starting materials [Fe₂{μ-C(OC₂H₅)-Ar}(CO)₄(η⁸-C₈H₈)], which is fluxional,^{3,9} suggesting that the COT ring is retained in these complexes.

The structure of complex **7** (Figure 1) resembles that of complex **5**,^{5c} except that the substituents at the carbene carbon and N atoms respectively are a C₆H₅

(9) For more detailed review about fluxional organometallics, see: Cotton, F. A. *Inorg. Chem.* **2002**, *41*, 643–658.

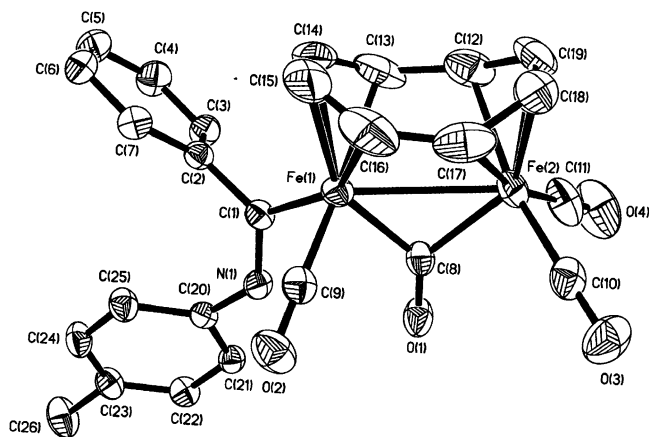


Figure 1. Molecular structure of **7**, showing the atom-numbering scheme with 45% thermal ellipsoids.

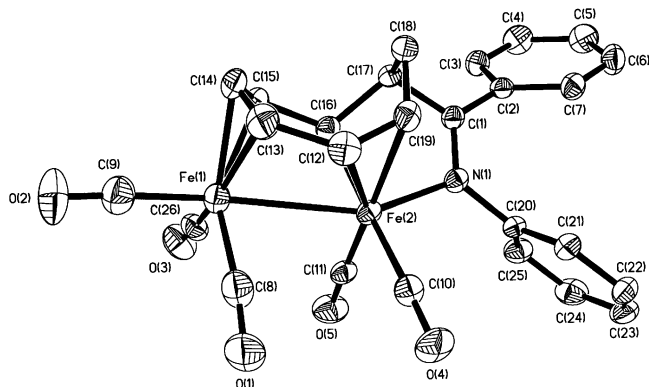


Figure 2. Molecular structure of **10**, showing the atom-numbering scheme with 40% thermal ellipsoids.

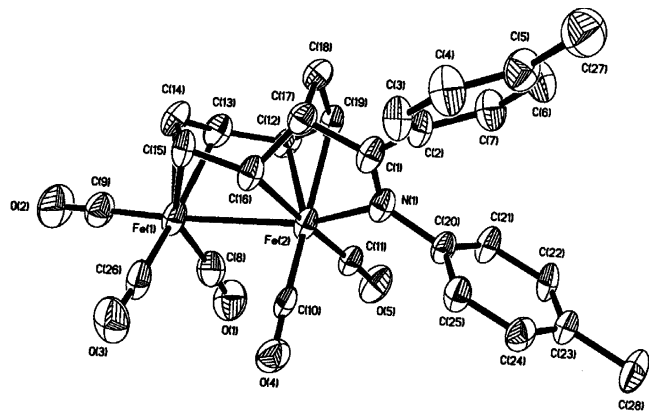


Figure 3. Molecular structure of **18**, showing the atom-numbering scheme with 45% thermal ellipsoids. Et₂O has been omitted for clarity.

and a *p*-CH₃C₆H₄ group in **7** but a *p*-CH₃C₆H₄ and a C₆H₅ group in the latter. Many structural features of **7** are very similar to those of **5**, as illustrated by the following parameters (the value for **7** is followed by the same parameters for **5**): Fe(1)–Fe(2) (2.7462(5), 2.7589–(19) Å), Fe(1)–C_{carbene} (1.913(2), 1.895(8) Å), C_{carbene}–N (1.328, 1.333(10) Å), average Fe(1)–C(COT) (2.166, 2.175 Å), average Fe(2)–C(COT) (2.151, 2.149 Å), average Fe–C(8) (1.932, 1.930 Å), Fe(1)–C(8)–Fe(2) (90.59–(4)°, 91.2(4)°). An apparent difference in the structures of **7** and **5** is the larger Fe(2)–Fe(1)–C(1) angle in **7** (129.94(7)°) as compared to **5** (127.1(3)°).

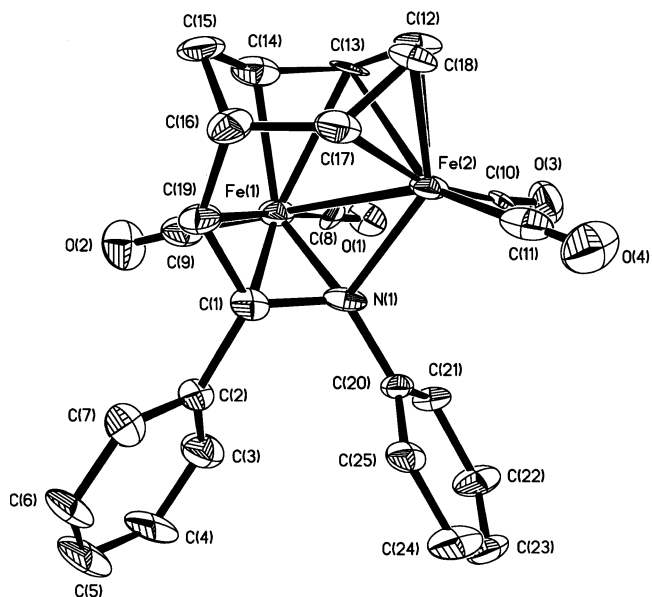


Figure 4. Molecular structure of **11**, showing the atom-numbering scheme with 45% thermal ellipsoids, showing only one of two independent molecules for clarity.

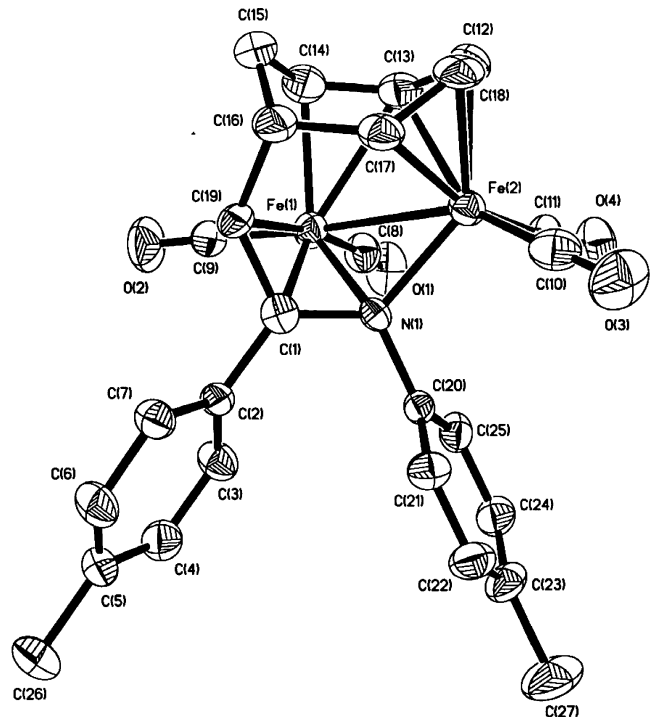
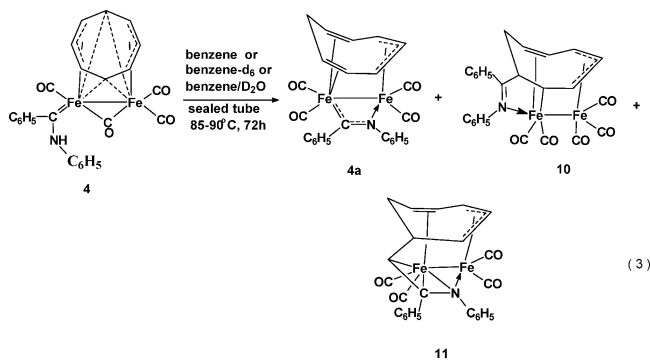


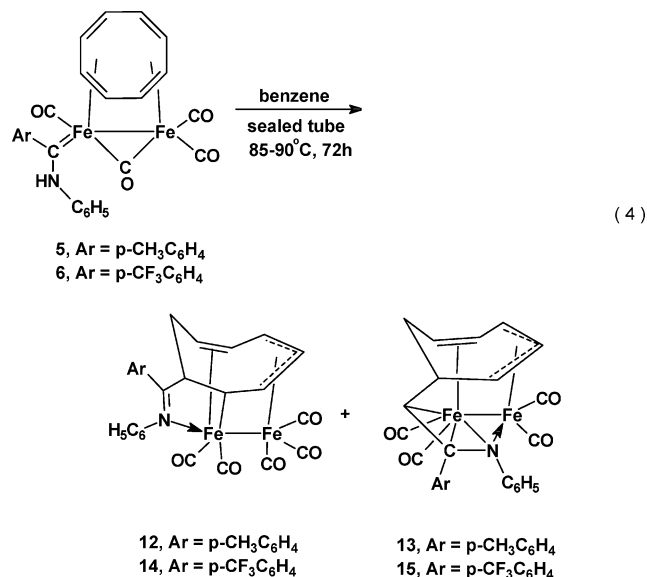
Figure 5. Molecular structure of **19**, showing the atom-numbering scheme with 45% thermal ellipsoids. CH₂Cl₂ has been omitted for clarity.

The possible reaction pathway to complexes **7–9** could be via an intermediate of [Fe₂{μ-C(Ar)NHC₆H₄CH₃-*p*}(CO)₄(η⁸-C₈H₈)] (Ar = C₆H₅ or *p*-CH₃C₆H₄ or *p*-CF₃C₆H₄), which was formed by the attack of the neutral *p*-CH₃C₆H₄NH₂ on the bridging carbene carbon of cationic bridging carbene complex **1** or **2** or **3** followed by deprotonation by the excess amine. Then the cleavage of the μ-C(1)–Fe(2) bond and the formation of the Fe(1)–C_{carbene} bond with bridging of a terminal CO ligand on Fe(1) to the Fe(2) atom could occur to produce complex **7** or **8** or **9**.

It is well known that the thermal decomposition of carbene complexes usually results in dimerization of the carbene ligand to produce alkene derivatives¹⁰ and that heating a Fischer-type carbene complex with an olefin generally results in the formation of the double-bond addition products.¹¹ What happens when the COT-coordinated diiron Fischer-type carbene complexes are subjected to thermolysis? To explore the thermolysis reactivity of the COT-coordinated diiron Fischer-type carbene complexes, we investigated the thermolysis reactions of complexes 4–8. A purple-red benzene solution of compound 4 in a sealed tube was heated with stirring at 85–90 °C for 72 h. After workup as described in the Experimental Section, a chelated diiron carbene complex $[\text{Fe}_2\{\text{C}(\text{C}_6\text{H}_5)\text{NC}_6\text{H}_5\}(\eta^2:\eta^3:\eta^2\text{-C}_8\text{H}_9)(\text{CO})_4]$ (**4a**), a novel C₈ ring addition product $[\text{Fe}_2\{\text{N}(\text{C}_6\text{H}_5)=\text{C}(\text{C}_6\text{H}_5)(\eta^1:\eta^3:\eta^2\text{-C}_8\text{H}_9)\}(\text{CO})_5]$ (**10**), and a novel C₇ contraction ring product $[\text{Fe}_2\{\text{N}(\text{C}_6\text{H}_5)=\text{C}(\text{C}_6\text{H}_5)\text{CH}(\eta^2:\eta^3\text{-C}_7\text{H}_8)(\text{CO})_4\}]$ (**11**) were obtained in 22–25%, 47–52%, and 10–11% yields, respectively (eq 3).

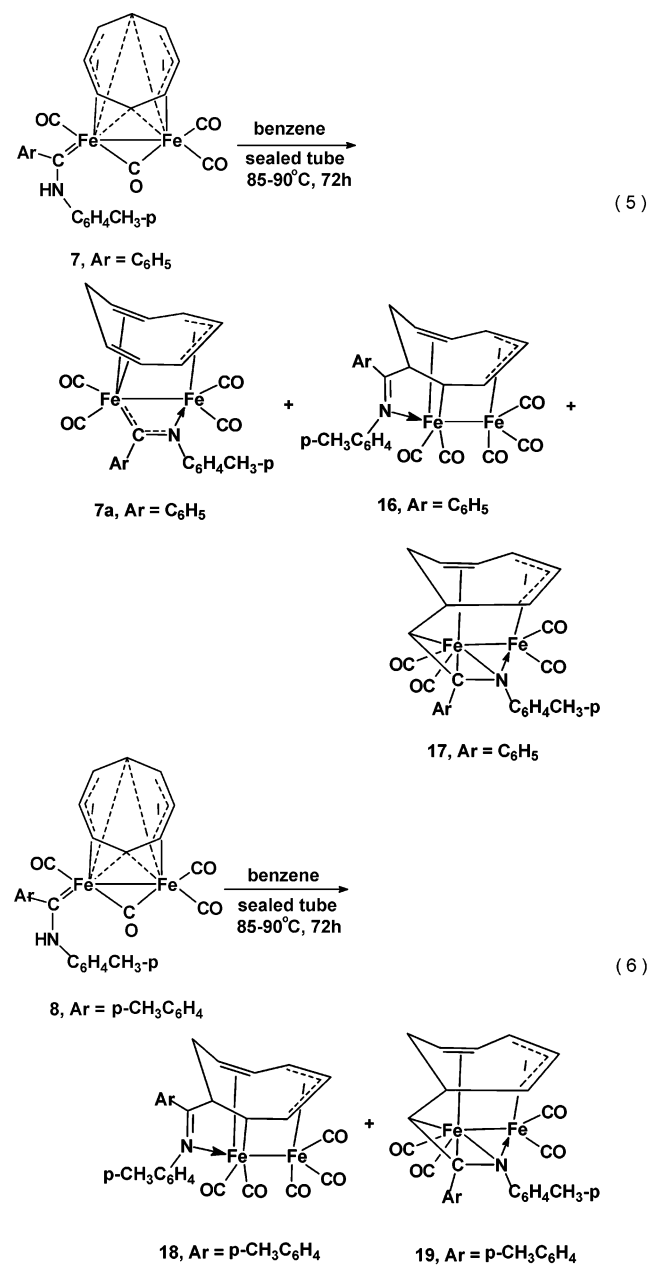


However, in the analogous thermolysis of complexes **5** and **6**, only the corresponding C₈ ring addition products $[\text{Fe}_2\{\text{N}(\text{C}_6\text{H}_5)=\text{C}(\text{Ar})(\eta^1:\eta^3:\eta^2\text{-C}_8\text{H}_9)\}(\text{CO})_5]$ (**12**, Ar = *p*-CH₃C₆H₄; **14**, Ar = *p*-CF₃C₆H₄) and C₇ contraction ring products $[\text{Fe}_2\{\text{N}(\text{C}_6\text{H}_5)=\text{C}(\text{Ar})\text{CH}(\eta^2:\eta^3\text{-C}_7\text{H}_8)(\text{CO})_4\}]$ (**13**, Ar = *p*-CH₃C₆H₄; **15**, Ar = *p*-CF₃C₆H₄) (eq 4) were isolated in 38–47% and 8–11% yields, respectively.



Similar to the thermolysis of **4**, the thermal decomposition of complex **7** under the same conditions as those

for **4–6** produced the analogous chelated diiron carbene complex $[\text{Fe}_2\{\text{C}(\text{C}_6\text{H}_5)\text{NC}_6\text{H}_4\text{CH}_3\text{-}p\}(\eta^2:\eta^3:\eta^2\text{-C}_8\text{H}_9)(\text{CO})_4]$ (**7a**), C₈ ring addition product $[\text{Fe}_2\{\text{N}(\text{C}_6\text{H}_4\text{CH}_3\text{-}p)=\text{C}(\text{C}_6\text{H}_5)(\eta^1:\eta^2:\eta^3\text{-C}_8\text{H}_9)\}(\text{CO})_5]$ (**16**), and C₇ contraction ring product $[\text{Fe}_2\{\text{N}(\text{C}_6\text{H}_4\text{CH}_3\text{-}p)=\text{C}(\text{C}_6\text{H}_5)\text{CH}(\eta^2:\eta^3\text{-C}_7\text{H}_8)\}(\text{CO})_4]$ (**17**) (eq 5) in 33, 28, and 10% yields, respectively. Like complexes **5** and **6**, the thermolysis of **8** under the same conditions yielded the corresponding C₈ ring addition product $[\text{Fe}_2\{\text{N}(\text{C}_6\text{H}_4\text{CH}_3\text{-}p)=\text{C}(\text{C}_6\text{H}_4\text{-CH}_3\text{-}p)(\eta^1:\eta^2:\eta^3\text{-C}_8\text{H}_9)\}(\text{CO})_5]$ (**18**) and C₇ contraction ring product $[\text{Fe}_2\{\text{N}(\text{C}_6\text{H}_4\text{CH}_3\text{-}p)=\text{C}(\text{C}_6\text{H}_4\text{CH}_3\text{-}p)\text{CH}(\eta^2:\eta^3\text{-C}_7\text{H}_8)\}(\text{CO})_4]$ (**19**) (eq 6) in 41 and 8% isolated yields, respectively.



Products **10–19** are sensitive to air in solution but relatively stable in the solid state. On the basis of elemental analyses and spectroscopic evidence, as well as X-ray crystallography, compounds **10**, **12**, **14**, **16**, and **18** are formulated as the eight-membered ring addition products. In these products, the original carbene ligand C(Ar)NHA_r' (Ar = C₆H₅ or *p*-CH₃C₆H₄ or *p*-CF₃C₆H₄;

Ar' = C₆H₅ or *p*-CH₃C₆H₄) is now a C(Ar)N(Ar') group formed by a H transfer from the N atom of the anilino to the C₈ ring, which is bonded to a carbon of the C₈ ring though the "carbene" carbon and coordinated to an Fe atom though the N atom. Products **11**, **13**, **15**, **17**, and **19** are formulated as the seven-membered ring contraction products, in which the cycloolefin ligand is now a seven-membered ring carrying a CHC(Ar)N(Ar') (Ar = C₆H₅ or *p*-CH₃C₆H₄ or *p*-CF₃C₆H₄; Ar' = C₆H₅ or *p*-CH₃C₆H₄) group with the two carbon atoms bonded to an Fe atom and the N atom to the two Fe atoms.

The IR and ¹H NMR spectra of complexes **10**–**19** are fully consistent with their structures shown in eqs 3–6 (Experimental Section). The structures of products **10**, **12**, **14**, **16**, and **18** and products **11**, **13**, **15**, **17**, and **19** were further confirmed by X-ray diffraction studies of complexes **10** and **18** and complexes **11** and **19**, respectively. The results of the X-ray diffraction work for complexes **10**, **11**, **18**, and **19** are summarized in Table 1, and their structures are shown in Figures 2–5, respectively.

The crystallographic investigation of **10** reveals an unusual structure (Figure 2). The eight-membered ring of the COT ligand is retained, but the COT ring has transformed into a C₈H₉ ring carrying a C(C₆H₅)NC₆H₅ group on C(17) with the coordination of the N atom to the Fe(2) atom, and the planarity of the COT ring has been destroyed to become a boat form configuration caused by the transfer of carbene ligand C(C₆H₅)-NHC₆H₅ from the Fe(2) atom to the C(17) atom of the C₈ ring accompanied by a H transfer from the N atom to the C(18) of the C₈ ring. Atoms C(13), C(4), and C(15) form an allyl-type unit η³-bonded to Fe(1), while the C(12) and C(19) atoms are η²-bonded to Fe(2), C(16) is σ bound to Fe(2), and a CO group generated from the decomposition of starting **4** or an intermediate is also bonded to the Fe(1) atom, thereby satisfying the 18-electron rule for both Fe atoms. The Fe–Fe bond distance (2.7599(7) Å) is slightly longer than that of **7** (2.7462(5) Å) but is significantly longer than that in **4a** (2.6920(9) Å).^{5b} The average Fe(1)–C bond length of C(13), C(14), and C(15) is 2.109 Å, and the average Fe(2)–C bond length of C(12), C(16), and C(19) is 2.168 Å. The C(1)–N(1) bond length of 1.288(3) Å is somewhat shorter than that found in **4a** (1.296(5) Å)^{5b} and **7** (1.328(3) Å), indicating high double-bond character. The very interesting structural feature of complex **10** is the C₈H₉ ligand. In **10**, the eight-membered ring is no longer planar and the bond distances have changed. In contrast to the planar eight-membered ring of **7**, only C(12), C(13), C(15), and C(16) are in a plane (±0.0017 Å); the C(14) atom is out of the C(12)C(13)C(15)C(16) plane by 0.2988 Å, while the C(17) and C(19) atoms are out of this plane by 1.2912 and 0.8616 Å, respectively. Another measure of the nonplanarity of the C₈H₉ eight-membered ring is the 27.02° dihedral angle between C(13), C(14), C(15) and C(12), C(13), C(15), C(16) planes and the 75.62° and 48.66° angles between the C(17), C(18), C(19) and C(12), C(13), C(15), C(16) planes and the C(17), C(18), C(19) and C(13), C(14), C(15) planes, respectively. The nonplanarity of the C₈H₉ ring in **10**

suggests that the π-system is not delocalized in the complex as it is in **7**. Another indication is the change in bond distances in **10** as compared to **7**. In contrast to the nearly equal bond distances in C(12) to C(19) of the eight-membered ring in **7**, in **10** the C(15)–C(16) (1.478(4) Å), C(16)–C(17) (1.527(4) Å), C(17)–C(18) (1.546(4) Å), and C(18)–C(19) (1.493(5) Å) bonds are considerably longer than C(12)–C(13) (1.454(5) Å), C(13)–C(14) (1.408(5) Å), C(14)–C(15) (1.382(5) Å), and C(12)–C(19) (1.362(5) Å).

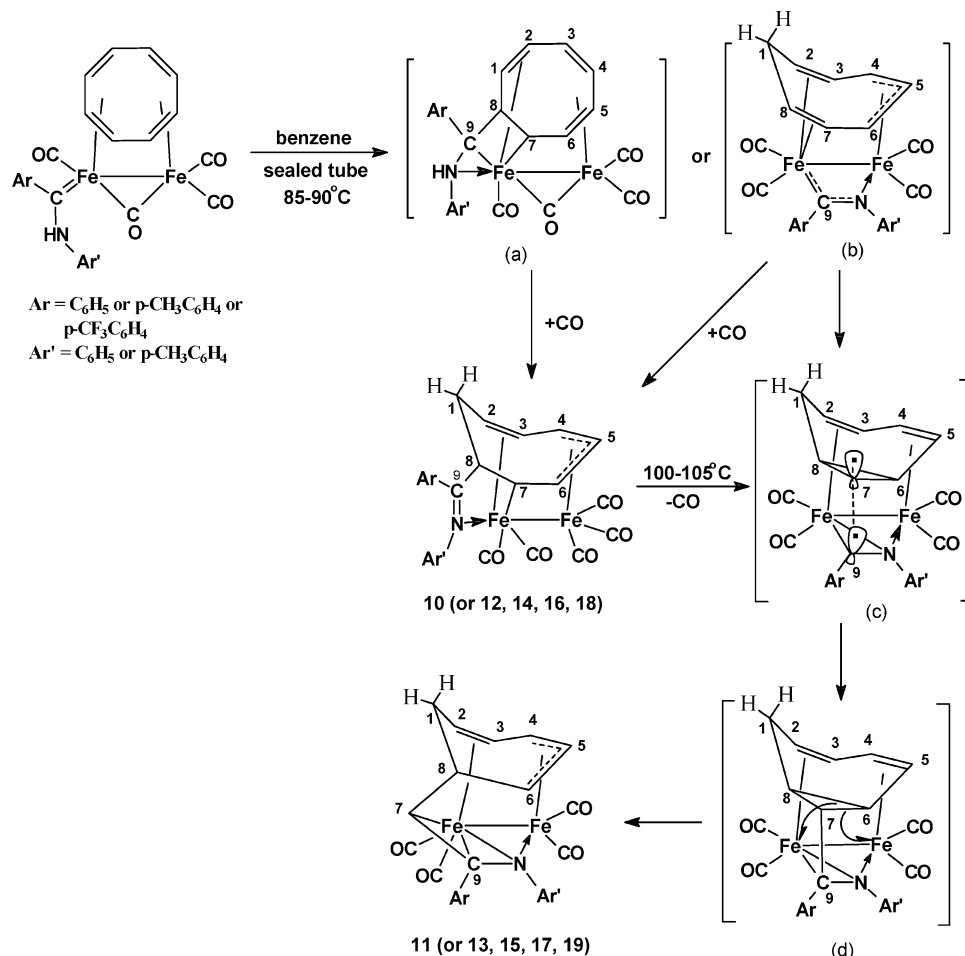
The structure of complex **18** shown in Figure 3 is very similar to that of **10**, except that the substituents on the C(1) and N(1) atoms are the two *p*-tolyl groups in **18** but the two phenyl groups in **10**. Interestingly, there are two independent molecules in the asymmetric unit of complex **18**. However, its ¹H NMR spectrum showed that the two molecules are separated in solution, giving a single normal molecule. The two molecules in the unit cell are the same. Many structural features of **18** are essentially the same as those in **10**: the Fe–Fe distance, the Fe(1)–C bond lengths of C(13), C(14), and C(15), the Fe(2)–C distances of C(12), C(16), and C(19), the bond distance of C(1)–N(1), the dihedral angle between the C(13)C(14)C(15) and the C(12)C(13)C(15)C(16) planes.

The crystallographic investigations of complexes **11** and **19** reveal also highly unusual structures. Both complexes are of the seven-membered ring η⁵-coordinated diiron alkyl complexes, in which the C(12), C(17), and C(18) atoms form an allyl-type unit η³-bonded to Fe(2), and the C(13) and C(14) atoms are η²-bonded to Fe(1). The C₇H₈ ring carries a CHC(Ar)N(Ar') (Ar = C₆H₅ or *p*-CH₃C₆H₄) group on C(16) with the C(1) and C(19) atoms bonded to Fe(1) in σ bond and the N(1) atom to Fe(1) and Fe(2), giving each Fe atom the 18-electron configuration. It is likely interesting that there are two independent enantiomorph molecules in the asymmetric unit of complex **11** and the two molecules in the unit cell are the same, similar to that of **18**. The molecular structures of complexes **11** and **19** shown in Figures 4 and 5, respectively, have many common features. The Fe–Fe bond distances in **11** and **19** are 2.671(4) and 2.6912(14) Å, respectively, which are somewhat shorter than that found in complex **7** and complexes **10** and **18**. The Fe(2)–C bond lengths of C(12), C(17), and C(18) are respectively 2.034(15), 2.089(16), and 2.030(17) Å in **11** and 2.062(7), 2.088(7), and 2.047(7) Å in **19**, while the Fe(1)–C bond lengths of C(13) and C(14) are respectively 2.378(13) and 2.098(16) Å in **11** and 2.400(8) and 2.115(8) Å in **19**. The C(1)–N(1) bond length of 1.390(15) Å for **11** and of 1.387(8) Å for **19** are C–N single bonds, which are somewhat longer than that in **4a** (1.296(5) Å)^{5b} by ca. 0.10 Å. The Fe(1)–N and Fe(2)–N distances are respectively 1.983(12) and 1.999(11) Å in **11** and 1.994(5) and 1.971(5) Å in **19**, which are slightly longer than that in **4a** (Fe(2)–N = 1.957(3) Å).^{5b} The C₇H₈ ring in **11** and **19** has a boat form configuration. The dihedral angles between the C(13), C(14), C(16), C(17) and C(14), C(15), C(16) planes and the C(13), C(14), C(16), C(17) and C(12), C(13), C(17), C(18) planes are respectively 60.95° and 29.71° in **11** and 55.35° and 34.67° in **19**. The benzene ring C(2)C(3)C(4)C(5)C(6)C(7) plane is oriented at an angle of 60.22° for **11** and of 55.25° for **19** with respect to the benzene ring C(20) through C(25) plane. An apparent

(10) Doetz, K. H. *Angew. Chem., Int. Ed. Engl.* **1984**, *23*, 587.

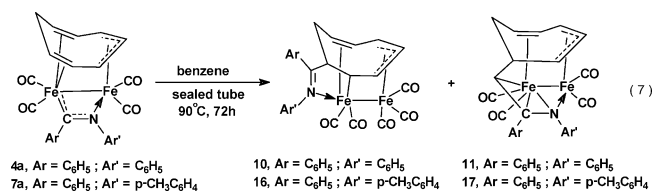
(11) Schubert, U. *Advances in Metal Carbene Chemistry*; Kluwer Academic Publishers: Norwell, 1988.

Scheme 1. Possible Mechanism for the Thermolysis of COT-Coordinated Diiron Carbene Complexes



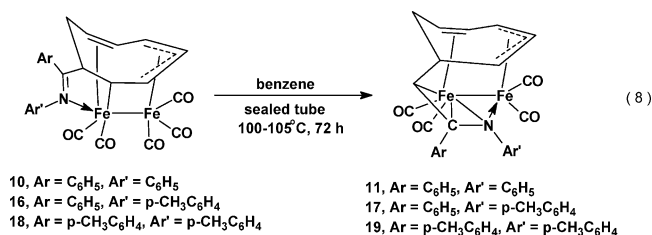
difference in the structures of **11** and **19** is the longer C(1)–C(19) (1.423(9) Å), C(14)–C(15) (1.536(11) Å), and C(16)–C(19) (1.536(10) Å) bonds and larger N(1)–C(1)–C(2) angle (124.0(6)°) in **19**, as compared with **11** (C(1)–C(19) = 1.395(19) Å, C(14)–C(15) = 1.47(2) Å, C(16)–C(19) = 1.496(10) Å, N(1)–C(1)–C(2) = 120.8(11)°).

Interestingly, the chelated carbene complexes **4a** and **7a** were transformed into the eight-membered ring addition products **10** and **16** and seven-membered ring products **11** and **17**, respectively, under the same conditions as those of complexes **4–8**. Heating the solution of compounds **4a** and **7a** in benzene in a sealed tube at 90 °C for 72 h as described in the Experimental Section gave the C₈ ring addition products **10** and **16** in 52 and 43% yields and the C₇ contraction ring products **11** and **17** in 10 and 9% yields, respectively (eq 7).



Surprisingly, the eight-membered ring compounds **10**, **16**, and **18** can also be partially transformed into the C₇ contraction ring products **11**, **17**, and **19**, respectively, by further thermolysis at relatively high thermolysis temperature (100–105 °C). A benzene solution of compounds **10**, **16**, and **18** respectively in a sealed tube was

heated to 100–105 °C for 72 h. After workup as described in the Experimental Section, the C₇ contraction ring products **11**, **17**, and **19** (eq 8) were obtained in 11, 9, and 10% yields, respectively.



Although a mechanism for the formation of the products **10**, **12**, **14**, **16**, and products **11**, **13**, **15**, **17**, and **19** has not yet been fully established, it seems possible via a metacyclobutane intermediate (a) or a chelated carbene intermediate (b) (Scheme 1). The former was formed by a [2 + 2] cycloaddition, similar to that of the ring-opened polyene complexes [MFe{C₈H₇(OC₂H₅)Ar}(CO)₆] (M = Mn, Re).^{12,13} For such an intermediate (a), a H shift from the N atom of the anilino to the C-1 position of the COT ring accompanied by the dissociation of the Fe–C(9) bond to form the C=N double bond and subsequent abstraction of one CO

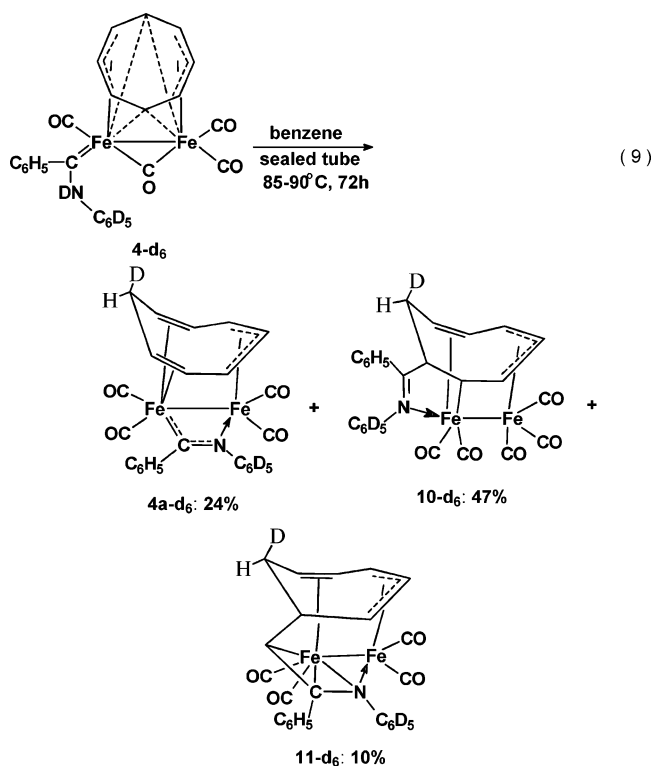
(12) Wang, B.-H.; Li, R.-H.; Sun, J.; Chen, J.-B. *J. Chem. Soc., Chem. Commun.* **1998**, 631.

(13) Xiao, N.; Zhang S.; Qiu, Z.-L.; Li, R.-H.; Wang, B.-H.; Xu, Q.; Sun, J.; Chen, J.-B. *Organometallics* **2002**, *21*, 3709.

molecule generated from the decomposition of the starting compound or an intermediate could occur to produce the C₈ ring addition product **10** (or **12**, **14**, **16**, and **18**). Of particular interest is the formation of the seven-membered ring compounds **11**, **13**, **15**, **17**, and **19**, which could be via an intermediate (b), namely a chelated diiron carbene complex. Actually, the easy transformation of the diiron carbene complexes into the more stable chelated carbene complexes has been previously confirmed by their solution ¹H NMR spectra and the isolation of the chelated carbene complexes from the CH₂Cl₂ solution.^{5b,c}

Strong evidence for the formation of intermediates (b) is that we have isolated the chelated diiron carbene complexes **4a** (eq 3) and **7a** (eq 5) from the thermolysis of complexes **4** and **7**, respectively. Under heating condition, the Fe atom (Fe(1)) in intermediates (b) could bond to the N atom, forming an Fe–N single bond, and the C(6), C(7), and C(8) atoms of the C₈ ring formed a three-membered ring to yield an intermediate (c), in which the C(7) and C(8) atoms each have one π electron. The new C(7)–C(9) bond could form by coupling of the two π electrons to give another intermediates (d). The latter then converted into the C₇ contraction ring product **11** (or **13**, **15**, **17**, and **19**) upon homolysis of the C(6)–C(7) bond. The reaction pathway to the C₈ ring addition product **10** (or **12**, **14**, **16**, and **18**) could also proceed via the intermediates (b) by abstracting one molecule of CO generated from the decomposition of the starting compound or an intermediate (Scheme 1). This has been confirmed by the experimental fact that when the benzene solution of **4a** or **7a** in a sealed tube was heated at 90 °C for 72 h, the C₈ ring addition product **10** or **16**, as main product, was obtained (eq 7), while the formation pathway from the C₈ ring addition products to the C₇ contraction ring products could proceed via the intermediates (c) and (d) by losing a CO ligand from the C₈ ring compounds at higher thermolysis temperature (100–105 °C), in which the cleavage of the C–C bond and formation of the C₇ ring are concerned, as shown in Scheme 1.

For the formation of the all thermolysis products, the transfer of one hydride to the COT ring would be the first step. Therefore, to confirm the hydride transfer and its source, the deuterated diiron carbene complex [Fe₂{=C(C₆H₅)NDC₆D₅}(μ-CO)(CO)₃(η⁸-C₈H₈)] (**4-d₆**) was prepared from deuterated aniline (C₆D₅ND₂) and **1** and used for the thermolysis instead of **4**. Interestingly, the thermolysis of **4-d₆** afforded the deuterated chelated carbene complex **4a-d₆**, deuterated C₈ ring addition product **10-d₆**, and deuterated C₇ contraction ring product **11-d₆** with about 80% deuterium incorporation (eq 9). Their ¹H NMR spectra clearly showed the positions of those deuteriums in **4a-d₆**, **10-d₆**, and **11-d₆**. (Compounds **4a-d₆**, **10-d₆**, and **11-d₆** each showed eight sets of signals for the C₈ or C₇ ring ligand and a much weaker signal assigned to an added H on the C-1 position of the C₈ or C₇ ring at δ 2.76 (m, 0.2H), 2.13 (dd, 0.2H), and 1.86 (m, 0.2H), respectively, which are derived from a little N-undeuterated impurity of [Fe₂{=C(C₆H₅)NHC₆D₅}(μ-CO)(CO)₃(η⁸-C₈H₈)] in starting **4-d₆** (Experimental Section).) This indicates that the added H atoms at the C-1 position of the C₈ and C₇ rings in **4a**, **10**, and **11** are from the H at N atom of the anilino



group of **4**. Further experimental evidence for the hydride transfer from the anilino to the COT ring is as follows: An acetone-*d*₆ solution of **4-d₆**, whose ¹H NMR spectrum had been measured which showed a single-line signal for the COT ring at 4.39 ppm, was kept at room temperature for 20–30 min. During this time the solution turned from deep red to red, and its ¹H NMR spectrum now showed eight sets of proton signals for the C₈ ring and a very weak signal at δ 2.76 (m, 0.2H), arising from the N-undeuterated impurity in **4-d₆**. This clearly indicates that the hydride (D) transfer from the N atom of the deuterated anilino to the COT ring occurred to form the deuterated chelated carbene complex **4a-d₆**.

To undoubtedly establish the source of an added H atom on the C-1 position of the C₈ and C₇ rings, the thermolysis of **4** in benzene-*d*₆ (C₆D₆) or in benzene containing deuterium oxide (D₂O) was carried out under the same conditions as those in benzene (eq 3), which afforded products **4a**, **10**, and **11**, the same products as those for the thermolysis of **4** in benzene, indicating that no deuterium (D) transfer from the solvent C₆D₆ or D₂O to the COT ring occurred. This excluded the possibility of the hydrogen being abstracted from benzene or water, which is a trace contaminant in solvent benzene or from glassware, and further demonstrated that the only origin of the added H atoms on the C-1 position of the C₈ and C₇ rings is the hydride at the N atom of the anilino in the starting compounds.

It is noteworthy that the yields of the C₇ ring products are relatively low (8–11%) in almost all the thermolysis reactions (eqs 3–8). Raising the thermolysis temperature or prolonging the heating time does not increase the yields of the C₇ contraction ring products but leads to the decomposition of the starting compounds and increases the unidentified decomposition products. This might be explained by the fact that the CO atmosphere generated by decomposition of the starting compounds

or an intermediate formed in the sealed tube favors the formation and existence of the C₈ ring addition products.

In summary, we have found remarkable thermolysis reactions of the COT-coordinated diiron Fischer-type carbene complexes, and a series of novel C₈ ring addition products and C₇ contraction ring products were obtained. A preliminary mechanistic study of these thermolysis reactions is also performed.

Acknowledgment. We thank the National Natural Science Foundation of China, the Science Foundation

of the Chinese Academy of Sciences, and the JSPS of Japan for financial support of this research.

Supporting Information Available: Tables of positional parameters and $B_{\text{iso}}/B_{\text{eq}}$, H atom coordinates, anisotropic displacement parameters, complete bond lengths and angles, and least-squares planes for **7**, **10**, **11**, **18**, and **19**. This material is available free of charge via the Internet at <http://pubs.acs.org>.

OM040101W